Computer Modeling in Engineering & Sciences CMES, vol.121, no.1, pp.215-247, 2019

3-D Thermo-Stress Field in Laminated Cylindrical Shells

Hai Qian[1, *], Sai-Huen Lo[2], Ding Zhou[3] and Yang Yang[1]

Abstract: The temperature and the stress distribution in simply-supported laminated cylindrical shells undergo thermal loads on the surface have been investigated. Exact solutions of physical quantities including temperature, heat flux, thermal displacement and stress are developed for the cylindrical laminated shell. Cylindrical shells are partitioned into more thin layers. In cylindrical coordinate, analytical expressions for physical quantities inside each layer are derived. Taking into account the compatibility of physical quantities at the interfaces, the relations between the outer and the inner layer of the laminated shell can be described with a transfer matrix. The undetermined parameters from the solutions of each layer can be obtained with boundary conditions. The convergence of the solutions to the number of Fourier series terms has been checked. The accuracy and feasibility of the present method is verified by comparing theoretical results with numerical outcomes due to Finite Element Method (FEM). Finally, the influences of surface temperature, geometrical size and material properties with respects to temperature, thermal stresses and displacement of layered cylindrical shell are worked out in details in a parameter study.

Keywords: Laminated cylindrical shells, thermo-elasticity, analytical solutions, transfer matrix.

1 Introduction

The mechanical responses of layered cylindrical shells have attracted considerable research efforts due to their increasing applications in the transportation of liquid and solid materials. Owing to the inhomogeneity of the laminated shell, complex stresses and deformations may be resulted even under a uniform temperature field. An accurate assessment of the displacement and the stress distribution in layered shell due to temperature loads would bring an important effect on the design and the structural safety of cylindrical pipes and other laminated composite cylindrical structures.

Lots of findings on temperature field of structural elements were presented before. Chang et al. [Chang, Kang and Chen (1973)] used Green's formulas to study steady and transient heat transfer in porous materials. Marin et al. [Marin and Lesnic (2007)] investigated the problems of steady heat conduction around nonlinear functionally graded

[1] Faculty of Civil Engineering and Mechanics, Jiangsu University, Zhenjiang, 212013, China.

[2] Department of Civil Engineering, University of Hong Kong, Hong Kong, China.

[3] College of Civil Engineering, Nanjing Tech University, Nanjing, 210009, China.

[*] Corresponding Author: Hai Qian. Email: ganensky@ujs.edu.cn.

materials (FGMs). Norouzi et al. [Norouzi, Delouei and Seilsepour (2013)] obtained exact solution for steady-state heat transfer in the fiber reinforced composite multilayered materials. Kayhani et al. [Kayhani, Norouzi and Delouei (2012)] adopted Sturm-Liouville theorem to derive the exact solution to investigate steady heat conduction in laminated cylinder. Tarn et al. [Tarn and Wang (2003)] used the state space approach to study the problem of heat conduction in anisotropic tube made by functional gradient materials. LU factorization approach is used by Kayhani et al. [Kayhani, Shariati, Nourozi et al. (2009)] to get an explicit solution of the steady heat conduction for composite laminated cylinder. Based on an equivalent single layer method, Blanc et al. [Blanc and Touratier (2007)] adopted equivalent single layer method and obtained an advanced exact model to solve the heat conduction problems for laminated structures. Ma et al. [Ma and Chang (2004)] developed a refined approach to solve the problem of heat conduction for anisotropic laminates. Haji-Sheikh et al. [Haji-Sheikh, Beck and Agonafer (2003)] derived an analytical solution to investigate steady heat conduction in double-layered objects. Rahideh et al. [Rahideh, Malekzadeh and Haghighi (2012)] simulated the heat conduction with finite wave heat speed in laminated FGM domain.

Thermal stresses on laminated structures have been widely studied by many researchers. Eason [Eason (1962)] studied time dependent thermal stress problems when the material is anisotropic. Ieşan [Ieşan (1980)] employed the linear thermo-elasticity theory and investigated the responses of laminated cylinder. Fard [Fard (2015)] showed exact analytical result to analyze a composite laminated panel under different boundary conditions according to an advanced sandwich panel theory. Aziz et al. [Aziz and Torabi (2013)] derived an exact solution of thermal stresses for hollow cylinder with constant interior heat generation and prescribed temperature conditions. Based on the thermo-elastic theory, Ruhi et al. [Ruhi, Angoshtari and Naghdabadi (2005)] obtained an analytical solution of laminated cylinders made by functionally graded materials. Ma et al. [Ma, Dui, Yang et al. (2015)] studied thermal displacements and stress from a hollow FGM sphere subjected to uniform thermal load and present an analytical solution. Hyer et al. [Hyer and Cooper (1986)] derived an analytical solution to solve the problem of composite pips under surrounding temperature gradient. Hyer et al. [Hyer, Cooper and Cohen (1986)] studied the influences of a constant temperature change on deformations and stresses in composite pipes. For the Green-Lindsay type objects, Hetnarski et al. [Hetnarski and Ignaczak (1993)] investigated the thermo-elastic waves induced by instantaneous heating-source. Ghugal et al. [Ghugal and Kulkarni (2013)] studied thermal stresses and displacements for orthotropic cross-ply multilayered plates with the theory of trigonometric shear deformation. Huang et al. [Huang and Tauchert (1992)] investigated the static response of a double-curved cross-ply composite plate subjected to mechanical and thermal loads. Ali et al. [Ali, Alsubari and Aminanda (2016)] provided an improved theory of shear deformation to investigate a laminated shell under hygrothermal and mechanical loads through simplifying this problem to such case of generalized plane strain deformations. On basis of Donnell's shell theory, Wu et al. [Wu, Jiang and Liu (2005)] studied the thermal buckling in multilayered shells made by FGMs. Javaheri et al. [Javaheri and Eslami (2002)] derived analytical solutions for the rectangular panel made by functional graded material subjected to thermal loads

according to the classic plate theory. Alankaya et al. [Alankaya and Oktem (2016)] studied the problem of static analysis of cross-ply double-curved shell on basis of an improved shear deformation theory. Chen et al. [Chen and Liu (2001)] studied thermal stress of the thin laminates with a boundary element method. Najafizadeh et al. [Najafizadeh and Eslami (2002)] discussed thermal buckling of circle panel made by FGMs on basis of an advanced shear deformation plate theory. With an asymptotic approach, Reddy et al. [Reddy and Cheng (2001)] studied 3D deformations in simply-supported plane made by FGMs. Shiah et al. [Shiah, Guao and Tan (2005)] developed BEM to analyze the thermal effects in 2D anisotropic material with heat sources. Kim et al. [Kim, Zhou and Chattopadhyay (2002)] established the thermal-piezoelectric-mechanical coupling model to study the distribution of interlaminar stress in smart laminated shells. Yas et al. [Yas and Aragh (2010)] discussed the 3D steady problem for the fiber rein-forced cylindrical panel made by FGMs. Kumar et al. [Kumar, Chakrabarti and Ketkar (2013)] provided static study of skew laminated shells with the theory of higher order shear deformation. Yuan [Yuan (1993)] provided an exact solution to discuss the thermal-induced responses of thick laminated shells under varying thermal load. Qian et al. [Qian, Zhou, Liu et al. (2014, 2015)] derived analytical solutions for simply-supported laminated plane undergoing different thermal loads. Moreover, Qian et al. [Qian, Zhou, Liu et al. (2015)] studied the simply-supported composite arches under steady thermal loads. On basis of refined shear deformation theory, Alankaya et al. [Alankaya and Erdonmez (2017)] used Double Fourier series to study the effects of curvature on hyperbolic paraboloidal formed, multilayered composite surfaces. With Galerkin finite element method, Ahmadi [Ahmadi (2017)] present a layer wise solution to investigate the distribution of stress in laminated plate under prescribed mechanical loads. Sladek et al. [Sladek, Sladek, Solek et al. (2008)] analyzed the thermal stresses in the Reissner-Mindlin shells with a meshless local Petrov-Galerkin approach. Civalek et al. [Civalek (2007); Civalek (2008); Civalek (2017); Civalek and Acar (2007)] studied free vibration in the conical panel, isotropic conical shells, carbon nanotubes reinforced, FG shell and plates, Mindlin plates on elastic foundations by discrete singular convolution. Bishay et al. [Bishay, Sladek, Sladek et al. (2012)] explored a new finite element to study MEE materials. Akgöz et al. [Akgöz and Civalek (2011)] studied nonlinear free vibration about thin laminates supported by non-linear elastic foundations. Zuo et al. [Zuo, Yang, Chen et al. (2014)] used a wavelet finite element to analyze FG plates with the Mindlin plate theory. Baltacıoglu et al. [Baltacıoglu, Akgöz and Civalek (2010)] studied large deflection of laminated plates. Xiang et al. [Xiang, Ma, Kitiornchai et al. (2002)] studied vibration in thin cylinders supported by intermediate ring and obtained an exact solution. Talebitooti [Talebitooti (2013)] studied free vibration in composite conical shells with LW-DQM. Wu et al. [Wu and Chi (2004)] presented an asymptotic theory to study nonlinear problem in laminated cylinders based on 3D nonlinear elastic theory. Wu et al. [Wu, Chiu and Wang (2008)] analyzed simply supported laminated piezoelectric plates based on the RKP method. Heydarpour et al. [Heydarpour, Malekzadeh, Haghighi et al. (2012); Heydarpour, Malekzadeh and Gholipour (2019); Heydarpour and Malekzadeh (2019)] used Lord-Shulman theory to study thermoelastic behavior of multi-FG spherical shells and FG-GPLRC spherical shells, and analyzed thermoelastic response of rotating FG cylinders with layerwise

differential quadrature method. Malekzadeh et al. [Malekzadeh and Ghaedsharaf (2014)] studied thermoelastic problem of laminated cylindrical panels according to 3D thermoelasticity theory. Malekzadeh et al. [Malekzadeh, Fiouz and Razi (2009)] presented a dynamic solution of laminated plates undergo moving load on the basis of 3D elasticity theory. Malekzadeh et al. [Malekzadeh and Beni (2015)] studied nonlinear free vibration of FG plates undergo different conditions.

Without the consideration of the effect of transverse shear deformation, the classic lamination theory with Love-Kirchhoff assumptions is a practical approach to assess the behavior of thin laminates. For thick laminates, the effect from transverse shear deformation should not be ignored. In this study, the 3D thermo-elasticity theory is applied to the laminated cylindrical shells under steady-state thermal loads on surfaces. The analytical solutions of each layer in laminated shells were developed with the help of transfer matrix method. Unlike one-layer equivalent approach, each layer of different material properties is dealt with separately, such that displacement and stresses at the interface are strictly compatible.

2 Temperature distributions over the cylinder

2.1 Temperature in a single shell layer

A laminated cylindrical shell consisted of P layers and the radius of the outer surface in jth layer is r_j (j=1, 2...P). The materials of each layer are isotropic. The geometry and the cylindrical coordinate system of the shell are presented in Fig. 1. The total length and the inner radius are represented by l and r_0, respectively. The material of each laminated layer is isotropic with possibly district to each other. The case is considered that the temperature of the two ends is a constant and this value is taken as the reference temperature. Without loss of generality, the temperatures are furtherly considered to be zero based on the relative temperature concept. The shell is simple-supported on boundaries. The inner and the outer surfaces are under thermal loads $t_1(\theta, z)$ and $t_p(\theta, z)$, respectively. Besides, we assume that the properties of materials are uninfluenced by the thermal process experienced by the shell.

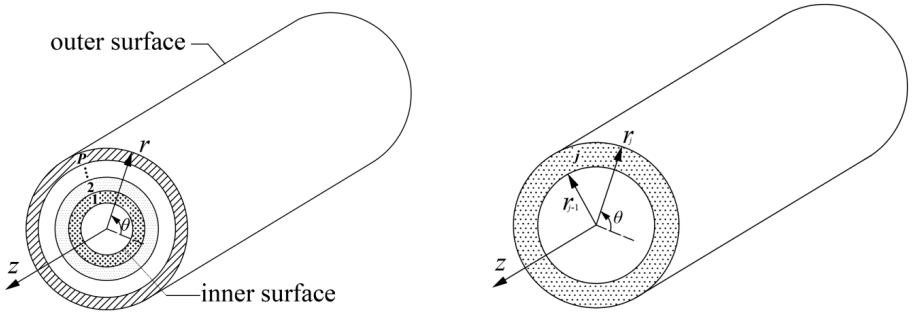

(a) multi-layer cylindrical shell (b) a homogenous layer of one material type

Figure 1: Model of multi-layer cylindrical shell

The thinning layer approach is introduced to solve the heat governing equation. As a result, each isotropic layer is further divided into M_j (j =1, 2… P) layers. Thus, the total layer-number is N ($N=\sum_{j=1}^{M} M_j$). In such case, the variable r in the heat governing equation can be approximately replaced by the center coordinate of layer r_{i0}. For thin layers, the heat conduction equation in the ith (i=1, 2 … N) layer can be given as

$$\frac{\partial^2 T_i(r,\theta,z)}{\partial r^2}+\frac{1}{r_{i0}}\frac{\partial T_i(r,\theta,z)}{\partial r}+\frac{1}{r_{i0}^2}\frac{\partial^2 T_i(r,\theta,z)}{\partial \theta^2}+\frac{\partial^2 T_i(r,\theta,z)}{\partial z^2}=0 \tag{1}$$

where r_{i0} is the center coordinate of the ith thin layer.

The temperature condition on the edges is

$$T_i\left(r,\theta,0\right)=T_i\left(r,\theta,l\right)=0\,. \tag{2}$$

The temperature distribution $T_i(r, \theta, z)$ can be given by the Fourier series

$$T_i(r,\theta,z)=\sum_{n=1}^{\infty} t_n^i(r)\sin\left(\frac{n\pi z}{l}\right)+\sum_{m=1}^{\infty}\sum_{n=1}^{\infty} a_{mn}^i(r)\cos(m\theta)\sin\left(\frac{n\pi z}{l}\right)+\sum_{m=1}^{\infty}\sum_{n=1}^{\infty} b_{mn}^i(r)\sin(m\theta)\sin\left(\frac{n\pi z}{l}\right). \tag{3}$$

The temperature solution (3) satisfies the temperature conditions (2). Substituting Eq. (3) into Eq. (1), $T_i(r,\theta,z)$ can be worked out as follows,

$$\begin{aligned} T_i\left(r,\theta,z\right)=&\sum_{n=1}^{\infty}\left(e^{\alpha_n^i r}H_{ni}^1+e^{\beta_n^i r}H_{ni}^2\right)\sin\left(\frac{n\pi z}{l}\right)+\sum_{m=1}^{\infty}\sum_{n=1}^{\infty}\left(e^{\alpha_{mn}^i r}H_{mni}^3+e^{\beta_{mn}^i r}H_{mni}^4\right)\cos\left(m\theta\right)\sin\left(\frac{n\pi z}{l}\right)\\ &+\sum_{m=1}^{\infty}\sum_{n=1}^{\infty}\left(e^{\alpha_{mn}^i r}H_{mni}^5+e^{\beta_{mn}^i r}H_{mni}^6\right)\sin\left(m\theta\right)\sin\left(\frac{n\pi z}{l}\right) \end{aligned} \tag{4}$$

where,

$$\alpha_n^i=\frac{\sqrt{\frac{4n^2\pi^2 r_{i0}^2}{l^2}+1}-1}{2r_{i0}},\qquad \beta_n^i=\frac{-\sqrt{\frac{4n^2\pi^2 r_{i0}^2}{l^2}+1}-1}{2r_{i0}},$$

$$\alpha_{mn}^i=\frac{\sqrt{4m^2+\frac{4n^2\pi^2 r_{i0}^2}{l^2}+1}-1}{2r_{i0}},\qquad \beta_{mn}^i=\frac{-\sqrt{4m^2+\frac{4n^2\pi^2 r_{i0}^2}{l^2}+1}-1}{2r_{i0}}, \tag{5}$$

and H_{ni}^1, H_{ni}^2, H_{mni}^3, H_{mni}^4, H_{mni}^5 and H_{mni}^6 are the unknown expressions of the ith layer. Once the coefficients are determined, the temperature filed of the laminated shell can be obtained.

2.2 Induction formulae of temperature

Based on Eq. (4), we can rewrite the temperature and the heat flux as matrix, i.e.,

$$\begin{bmatrix} T_i(r,\theta,z) \\ k_i \dfrac{\partial T_i(r,\theta,z)}{\partial r} \end{bmatrix} = \left[\psi_{mn}^i(r,\theta,z)\right] = \sum_{n=1}^{\infty}\left[\phi_n^i(r)\right]\sin\left(\frac{n\pi z}{l}\right) + \sum_{m=1}^{\infty}\sum_{n=1}^{\infty}\left[\phi_{mn1}^i(r)\right]\cos(m\theta)\sin\left(\frac{n\pi z}{l}\right) + \sum_{m=1}^{\infty}\sum_{n=1}^{\infty}\left[\phi_{mn2}^i(r)\right]\sin(m\theta)\sin\left(\frac{n\pi z}{l}\right) \tag{6}$$

where k_i is heat transfer coefficient, and $\left[\phi_n^i(r)\right]$, $\left[\phi_{mn1}^i(r)\right]$, $\left[\phi_{mn2}^i(r)\right]$ are 2×1 matrix function described as from temperature solution (4),

$$\left[\phi_n^i(r)\right] = \left[\varphi_n^i(r)\right]\left[\Lambda_n^i\right],\quad \left[\phi_{mn1}^i(r)\right] = \left[\varphi_{mn1}^i(r)\right]\left[\Lambda_{mn1}^i\right],\quad \left[\phi_{mn2}^i(r)\right] = \left[\varphi_{mn2}^i(r)\right]\left[\Lambda_{mn2}^i\right] \tag{7}$$

respectively,

in which,

$$\left[\varphi_n^i(r)\right] = \begin{bmatrix} e^{\alpha_n^i r} & e^{\beta_n^i r} \\ k_i\alpha_n^i e^{\alpha_n^i r} & k_i\beta_n^i e^{\beta_n^i r} \end{bmatrix},\quad \left[\Lambda_n^i\right] = \begin{bmatrix} H_{ni}^1 \\ H_{ni}^2 \end{bmatrix},\quad \left[\varphi_{mn1}^i(r)\right] = \begin{bmatrix} e^{\alpha_{mn}^i r} & e^{\beta_{mn}^i r} \\ k_i\alpha_{mn}^i e^{\alpha_{mn}^i r} & k_i\beta_{mn}^i e^{\beta_{mn}^i r} \end{bmatrix},$$

$$\left[\Lambda_{mn1}^i\right] = \begin{bmatrix} H_{mni}^3 \\ H_{mni}^4 \end{bmatrix},\quad \left[\varphi_{mn2}^i(r)\right] = \begin{bmatrix} e^{\alpha_{mn}^i r} & e^{\beta_{mn}^i r} \\ k_i\alpha_{mn}^i e^{\alpha_{mn}^i r} & k_i\beta_{mn}^i e^{\beta_{mn}^i r} \end{bmatrix},\quad \left[\Lambda_{mn2}^i\right] = \begin{bmatrix} H_{mni}^5 \\ H_{mni}^6 \end{bmatrix}. \tag{8}$$

Taking $r = r_i$ and $r = r_{i-1}$ in Eq. (7) respectively, the unknown coefficients $\left[\Lambda_n^i\right]$, $\left[\Lambda_{mn1}^i\right]$ and $\left[\Lambda_{mn2}^i\right]$ can be eliminated as follows,

$$\left[\phi_n^i(r_i)\right] = \left[\varphi_n^i(r_i)\right]\left[\varphi_n^i(r_{i-1})\right]^{-1}\left[\phi_n^i(r_{i-1})\right],\quad \left[\phi_{mn1}^i(r_i)\right] = \left[\varphi_{mn1}^i(r_i)\right]\left[\varphi_{mn1}^i(r_{i-1})\right]^{-1}\left[\phi_{mn1}^i(r_{i-1})\right],$$

$$\left[\phi_{mn2}^i(r_i)\right] = \left[\varphi_{mn2}^i(r_i)\right]\left[\varphi_{mn2}^i(r_{i-1})\right]^{-1}\left[\phi_{mn2}^i(r_{i-1})\right]. \tag{9}$$

Based on the continuity condition at the interface of the laminated shell, we have

$$\left[\psi_{mn}^i(r_i,\theta,z)\right] = \left[\psi_{mn}^{i+1}(r_i,\theta,z)\right]. \tag{10}$$

Therefore, the relations between the qth (q=2, 3…N) and the inner layers can be recursively obtained:

$$\begin{bmatrix} H_{nq}^1 \\ H_{nq}^2 \end{bmatrix} = \left[\varphi_n^q(r_q)\right]^{-1}\left\{\prod_{i=1}^{q}\left[\varphi_n^i(r_i)\right]\left[\varphi_n^i(r_{i-1})\right]^{-1}\right\}\left[\varphi_n^1(r_0)\right]\begin{bmatrix} H_{n1}^1 \\ H_{n1}^2 \end{bmatrix},$$

$$\begin{bmatrix} H_{mnq}^3 \\ H_{mnq}^4 \end{bmatrix} = \left[\varphi_{mn1}^q(r_q)\right]^{-1}\left\{\prod_{i=1}^{q}\left[\varphi_{mn1}^i(r_i)\right]\left[\varphi_{mn1}^i(r_{i-1})\right]^{-1}\right\}\left[\varphi_{mn1}^1(r_0)\right]\begin{bmatrix} H_{mn1}^3 \\ H_{mn1}^4 \end{bmatrix},$$

$$\begin{bmatrix} H_{mnq}^5 \\ H_{mnq}^6 \end{bmatrix} = \left[\varphi_{mn2}^q(r_q)\right]^{-1}\left\{\prod_{i=1}^{q}\left[\varphi_{mn2}^i(r_i)\right]\left[\varphi_{mn2}^i(r_{i-1})\right]^{-1}\right\}\left[\varphi_{mn2}^1(r_0)\right]\begin{bmatrix} H_{mn1}^5 \\ H_{mn1}^6 \end{bmatrix}. \tag{11}$$

2.3 Undetermined temperature coefficients

Think over that outer and inner surfaces of cylindrical shell under steady state thermal

loads $t_p(\theta, z)$ and $t_1(\theta, z)$,

$$T_1(r_0,\theta,z)=t_1(\theta,z),\quad T_N(r_N,\theta,z)=t_p(\theta,z). \tag{12}$$

The Fourier series can be adopted to express temperature loads $t_p(\theta, z)$ and $t_1(\theta, z)$,

$$\begin{aligned}
t_1(\theta,z)=&\sum_{n=1}^{\infty}\left[\frac{1}{\pi l}\int_{-\pi}^{\pi}\int_0^l t_1(\theta,z)\sin\left(\frac{n\pi z}{l}\right)dzd\theta\right]\sin\left(\frac{n\pi z}{l}\right)\\
&+\sum_{m=1}^{\infty}\sum_{n=1}^{\infty}\left[\frac{2}{\pi l}\int_{-\pi}^{\pi}\int_0^l t_1(\theta,z)\cos(m\theta)\sin\left(\frac{n\pi z}{l}\right)dzd\theta\right]\cos(m\theta)\sin\left(\frac{n\pi z}{l}\right)\\
&+\sum_{m=1}^{\infty}\sum_{n=1}^{\infty}\left[\frac{2}{\pi l}\int_{-\pi}^{\pi}\int_0^l t_1(\theta,z)\sin(m\theta)\sin\left(\frac{n\pi z}{l}\right)dzd\theta\right]\sin(m\theta)\sin\left(\frac{n\pi z}{l}\right),\\
t_p(\theta,z)=&\sum_{n=1}^{\infty}\left[\frac{1}{\pi l}\int_{-\pi}^{\pi}\int_0^l t_p(\theta,z)\sin\left(\frac{n\pi z}{l}\right)dzd\theta\right]\sin\left(\frac{n\pi z}{l}\right)\\
&+\sum_{m=1}^{\infty}\sum_{n=1}^{\infty}\left[\frac{2}{\pi l}\int_{-\pi}^{\pi}\int_0^l t_p(\theta,z)\cos(m\theta)\sin\left(\frac{n\pi z}{l}\right)dzd\theta\right]\cos(m\theta)\sin\left(\frac{n\pi z}{l}\right)\\
&+\sum_{m=1}^{\infty}\sum_{n=1}^{\infty}\left[\frac{2}{\pi l}\int_{-\pi}^{\pi}\int_0^l t_p(\theta,z)\sin(m\theta)\sin\left(\frac{n\pi z}{l}\right)dzd\theta\right]\sin(m\theta)\sin\left(\frac{n\pi z}{l}\right).
\end{aligned} \tag{13}$$

Substituting the temperature solution (4) into boundary Eqs. (12) and (13) gives

$$e^{\alpha_n^1 r_0}H_{n1}^1+e^{\beta_n^1 r_0}H_{n1}^2=\frac{1}{\pi l}\int_{-\pi}^{\pi}\int_0^l t_1(\theta,z)\sin\left(\frac{n\pi z}{l}\right)dzd\theta,$$

$$e^{\alpha_{mn}^1 r_0}H_{mn1}^3+e^{\beta_{mn}^1 r_0}H_{mn1}^4=\frac{2}{\pi l}\int_{-\pi}^{\pi}\int_0^l t_1(\theta,z)\cos(m\theta)\sin\left(\frac{n\pi z}{l}\right)dzd\theta,$$

$$e^{\alpha_{mn}^1 r_0}H_{mn1}^5+e^{\beta_{mn}^1 r_0}H_{mn1}^6=\frac{2}{\pi l}\int_{-\pi}^{\pi}\int_0^l t_1(\theta,z)\sin(m\theta)\sin\left(\frac{n\pi z}{l}\right)dzd\theta,$$

$$e^{\alpha_n^N r_N}H_{nN}^1+e^{\beta_n^N r_N}H_{nN}^2=\frac{1}{\pi l}\int_{-\pi}^{\pi}\int_0^l t_p(\theta,z)\sin\left(\frac{n\pi z}{l}\right)dzd\theta,$$

$$e^{\alpha_{mn}^N r_N}H_{mnN}^3+e^{\beta_{mn}^N r_N}H_{mnN}^4=\frac{2}{\pi l}\int_{-\pi}^{\pi}\int_0^l t_p(\theta,z)\cos(m\theta)\sin\left(\frac{n\pi z}{l}\right)dzd\theta,$$

$$e^{\alpha_{mn}^N r_N}H_{mnN}^5+e^{\beta_{mn}^N r_N}H_{mnN}^6=\frac{2}{\pi l}\int_{-\pi}^{\pi}\int_0^l t_p(\theta,z)\sin(m\theta)\sin\left(\frac{n\pi z}{l}\right)dzd\theta. \tag{14}$$

Solving Eq. (11) (taking q=N) and Eq. (14), H_{n1}^1, H_{n1}^2, H_{mn1}^3, H_{mn1}^4, H_{mn1}^5, H_{mn1}^6 and H_{nN}^1, H_{nN}^2, H_{mnN}^3, H_{mnN}^4, H_{mnN}^5, H_{mnN}^6 can all be determined. Substituting the coefficients of the first layer H_{n1}^1, H_{n1}^2, H_{mn1}^3, H_{mn1}^4, H_{mn1}^5 and H_{mn1}^6 back to Eq. (11), the unknown coefficients of the qth layer H_{nq}^1, H_{nq}^2, H_{mnq}^3, H_{mnq}^4, H_{mnq}^5 and H_{mnq}^6 (q=2, 3…N -1) can be determined in turn. At last, the temperature distribution can be derived out by taking these coefficients to the general solution of temperature field (4).

3 Displacement and stress distributions over the cylinder

3.1 Displacement in a single layer

The thermal expansion coefficient is denoted by α_i. The Young's modulus of each layer is denoted by E_i. The Poisson's ratio is denoted by μ_i. The thinning layer approach in Section 2.1 can also be employed in simplifying the three-dimensional thermo-elasticity equation. Thermo-elastic constitutive relationships of the ith layer (i=1, 2 … N) in the cylindrical coordinate system are given by

$$\sigma_r^i(r,\theta,z)=(\lambda_i+2G_i)\frac{\partial u_i(r,\theta,z)}{\partial r}+\lambda_i\left(\frac{1}{r_{i0}}\frac{\partial v_i(r,\theta,z)}{\partial\theta}+\frac{u_i(r,\theta,z)}{r_{i0}}\right)+\lambda_i\frac{\partial w_i(r,\theta,z)}{\partial z}-(3\lambda_i+2G_i)\alpha_i T_i(r,\theta,z),$$

$$\sigma_\theta^i(r,\theta,z)=(\lambda_i+2G_i)\left(\frac{1}{r_{i0}}\frac{\partial v_i(r,\theta,z)}{\partial\theta}+\frac{u_i(r,\theta,z)}{r_{i0}}\right)+\lambda_i\frac{\partial u_i(r,\theta,z)}{\partial r}+\lambda_i\frac{\partial w_i(r,\theta,z)}{\partial z}-(3\lambda_i+2G_i)\alpha_i T_i(r,\theta,z),$$

$$\sigma_z^i(r,\theta,z)=(\lambda_i+2G_i)\frac{\partial w_i(r,\theta,z)}{\partial z}+\lambda_i\frac{\partial u_i(r,\theta,z)}{\partial r}+\lambda_i\left(\frac{1}{r_{i0}}\frac{\partial v_i(r,\theta,z)}{\partial\theta}+\frac{u_i(r,\theta,z)}{r_{i0}}\right)-(3\lambda_i+2G_i)\alpha_i T_i(r,\theta,z),$$

$$\tau_{\theta z}^i(r,\theta,z)=G_i\left(\frac{1}{r_{i0}}\frac{\partial w_i(r,\theta,z)}{\partial\theta}+\frac{\partial v_i(r,\theta,z)}{\partial z}\right),\quad \tau_{rz}^i(r,\theta,z)=G_i\left(\frac{\partial u_i(r,\theta,z)}{\partial z}+\frac{\partial w_i(r,\theta,z)}{\partial r}\right),$$

$$\tau_{r\theta}^i(r,\theta,z)=G_i\left(\frac{\partial v_i(r,\theta,z)}{\partial r}+\frac{1}{r_{i0}}\frac{\partial u_i(r,\theta,z)}{\partial\theta}-\frac{v_i(r,\theta,z)}{r_{i0}}\right). \tag{15}$$

where $\tau_{\theta z}^i(r,\theta,z)$, $\tau_{rz}^i(r,\theta,z)$, $\tau_{r\theta}^i(r,\theta,z)$, $\sigma_r^i(r,\theta,z)$, $\sigma_\theta^i(r,\theta,z)$ and $\sigma_z^i(r,\theta,z)$ are stress of the ith layer (i=1, 2 … N), $u_i(r,\theta,z)$, $v_i(r,\theta,z)$ and $w_i(r,\theta,z)$ are displacement components, respectively. λ_i and G_i are the Lamè constants described as:

$$\lambda_i=\frac{\mu_i E_i}{(1+\mu_i)(1-2\mu_i)},\qquad G_i=\frac{E_i}{2(1+\mu_i)}. \tag{16}$$

The equilibrium equations without the body forces for the ith layer (i=1, 2, … N) can be written as

$$\frac{\partial\sigma_z^i(r,\theta,z)}{\partial z}+\frac{1}{r_{i0}}\frac{\partial\tau_{\theta z}^i(r,\theta,z)}{\partial\theta}+\frac{\partial\tau_{rz}^i(r,\theta,z)}{\partial r}+\frac{\tau_{rz}^i(r,\theta,z)}{r_{i0}}=0,$$

$$\frac{\partial\tau_{\theta z}^i(r,\theta,z)}{\partial z}+\frac{1}{r_{i0}}\frac{\partial\sigma_\theta^i(r,\theta,z)}{\partial\theta}+\frac{\partial\tau_{r\theta}^i(r,\theta,z)}{\partial r}+\frac{2\tau_{r\theta}^i(r,\theta,z)}{r_{i0}}=0,$$

$$\frac{\partial \tau_{rz}^{i}(r,\theta,z)}{\partial z}+\frac{1}{r_{i0}}\frac{\partial \tau_{r\theta}^{i}(r,\theta,z)}{\partial \theta}+\frac{\partial \sigma_{r}^{i}(r,\theta,z)}{\partial r}+\frac{\sigma_{r}^{i}(r,\theta,z)-\sigma_{\theta}^{i}(r,\theta,z)}{r_{i0}}=0. \tag{17}$$

Substituting thermo-elastic constitutive relationships (15) into Eq. (17), the equilibrium differential equations for displacements are given by

$$\begin{aligned}
&\left[(\lambda_i+2G_i)\frac{\partial^2 w_i(r,\theta,z)}{\partial z^2}+\lambda_i\frac{\partial^2 u_i(r,\theta,z)}{\partial r\partial z}+\lambda_i\left(\frac{1}{r_{i0}}\frac{\partial^2 v_i(r,\theta,z)}{\partial\theta\partial z}+\frac{1}{r_{i0}}\frac{\partial u_i(r,\theta,z)}{\partial z}\right)-(3\lambda_i+2G_i)\alpha_i\frac{\partial T_i(r,\theta,z)}{\partial z}\right]\\
&+\frac{G_i}{r_{i0}}\left(\frac{1}{r_{i0}}\frac{\partial^2 w_i(r,\theta,z)}{\partial\theta^2}+\frac{\partial^2 v_i(r,\theta,z)}{\partial z\partial\theta}\right)+G_i\left(\frac{\partial^2 u_i(r,\theta,z)}{\partial z\partial r}+\frac{\partial^2 w_i(r,\theta,z)}{\partial r^2}\right)+\frac{G_i}{r_{i0}}\left(\frac{\partial u_i(r,\theta,z)}{\partial z}+\frac{\partial w_i(r,\theta,z)}{\partial r}\right)=0,\\
&\frac{1}{r_{i0}}\left[(\lambda_i+2G_i)\left(\frac{1}{r_{i0}}\frac{\partial^2 v_i(r,\theta,z)}{\partial\theta^2}+\frac{1}{r_{i0}}\frac{\partial u_i(r,\theta,z)}{\partial\theta}\right)+\lambda_i\frac{\partial^2 u_i(r,\theta,z)}{\partial r\partial\theta}+\lambda_i\frac{\partial^2 w_i(r,\theta,z)}{\partial z\partial\theta}-\right.\\
&\left.(3\lambda_i+2G_i)\alpha_i\frac{\partial T_i(r,\theta,z)}{\partial\theta}\right]+G_i\left(\frac{\partial^2 v_i(r,\theta,z)}{\partial r^2}+\frac{1}{r_{i0}}\frac{\partial^2 u_i(r,\theta,z)}{\partial\theta\partial r}-\frac{1}{r_{i0}}\frac{\partial v_i(r,\theta,z)}{\partial r}\right)\\
&+\frac{2G_i}{r_{i0}}\left(\frac{\partial v_i(r,\theta,z)}{\partial r}+\frac{1}{r_{i0}}\frac{\partial u_i(r,\theta,z)}{\partial\theta}-\frac{v_i(r,\theta,z)}{r_{i0}}\right)+G_i\left(\frac{1}{r_{i0}}\frac{\partial^2 w_i(r,\theta,z)}{\partial\theta\partial z}+\frac{\partial^2 v_i(r,\theta,z)}{\partial z^2}\right)=0,\\
&\left[(\lambda_i+2G_i)\frac{\partial^2 u_i(r,\theta,z)}{\partial r^2}+\lambda_i\left(\frac{1}{r_{i0}}\frac{\partial^2 v_i(r,\theta,z)}{\partial\theta\partial r}+\frac{1}{r_{i0}}\frac{\partial u_i(r,\theta,z)}{\partial r}\right)+\lambda_i\frac{\partial^2 w_i(r,\theta,z)}{\partial z\partial r}-(3\lambda_i+2G_i)\alpha_i\frac{\partial T_i(r,\theta,z)}{\partial r}\right]\\
&+G_i\left(\frac{\partial^2 u_i(r,\theta,z)}{\partial z^2}+\frac{\partial^2 w_i(r,\theta,z)}{\partial r\partial z}\right)+\frac{G_i}{r_{i0}}\left(\frac{\partial^2 v_i(r,\theta,z)}{\partial r\partial\theta}+\frac{1}{r_{i0}}\frac{\partial^2 u_i(r,\theta,z)}{\partial\theta^2}-\frac{1}{r_{i0}}\frac{\partial v_i(r,\theta,z)}{\partial\theta}\right)\\
&+\frac{2G_i}{r_{i0}}\left(\frac{\partial u_i(r,\theta,z)}{\partial r}-\frac{1}{r_{i0}}\frac{\partial v_i(r,\theta,z)}{\partial\theta}-\frac{u_i(r,\theta,z)}{r_{i0}}\right)=0.
\end{aligned} \tag{18}$$

Since there is no in-plane displacement on both ends, we can obtain

$$u_i(r,\theta,0)=u_i(r,\theta,l)=0,\quad v_i(r,\theta,0)=v_i(r,\theta,l)=0. \tag{19}$$

The Fourier series can be adopted to describe the displacement as follows,

$$\begin{aligned}
u_i(r,\theta,z)&=\sum_{n=1}^{\infty}U_{n0}^{i}(r)\sin\frac{n\pi z}{l}+\sum_{m=1}^{\infty}\sum_{n=1}^{\infty}U_{mn1}^{i}(r)\cos(m\theta)\sin\frac{n\pi z}{l}+\sum_{m=1}^{\infty}\sum_{n=1}^{\infty}U_{mn2}^{i}(r)\sin(m\theta)\sin\frac{n\pi z}{l},\\
v_i(r,\theta,z)&=\sum_{n=1}^{\infty}V_{n0}^{i}(r)\sin\frac{n\pi z}{l}+\sum_{m=1}^{\infty}\sum_{n=1}^{\infty}V_{mn1}^{i}(r)\sin(m\theta)\sin\frac{n\pi z}{l}+\sum_{m=1}^{\infty}\sum_{n=1}^{\infty}V_{mn2}^{i}(r)\cos(m\theta)\sin\frac{n\pi z}{l},\\
w_i(r,\theta,z)&=w_i(r,\theta)+\sum_{n=1}^{\infty}W_{n0}^{i}(r)\cos\frac{n\pi z}{l}\\
&\quad+\sum_{m=1}^{\infty}\sum_{n=1}^{\infty}W_{mn1}^{i}(r)\cos(m\theta)\cos\frac{n\pi z}{l}+\sum_{m=1}^{\infty}\sum_{n=1}^{\infty}W_{mn2}^{i}(r)\sin(m\theta)\cos\frac{n\pi z}{l}.
\end{aligned} \tag{20}$$

in which $U_{n0}^{i}(r)$, $U_{mn1}^{i}(r)$, $U_{mn2}^{i}(r)$, $V_{n0}^{i}(r)$, $V_{mn1}^{i}(r)$, $V_{mn2}^{i}(r)$, $W_{n0}^{i}(r)$, $W_{mn1}^{i}(r)$ and $W_{mn2}^{i}(r)$ are the undetermined expressions in r, while $w_i(r,\theta)$ is the unknown functions in r and θ. Eq. (20) satisfies the boundary conditions of Eq. (19). Here, $w_i(r,\theta,z)$ can be decomposed into two parts.

3.1.1 Case 1: n=0

When n=0, $w_i(r,\theta,z)$=$w_i(r,\theta)$. In this case, we have

$$T_i(r,\theta,z)=0,\ u_i(r,\theta,z)=0,\ v_i(r,\theta,z)=0. \tag{21}$$

Substituting solution (21) into the equilibrium differential Eq. (18), a partial differential equation of second order is obtained:

$$\frac{1}{r^2}\frac{\partial^2 w_i(r,\theta)}{\partial\theta^2}+\frac{\partial^2 w_i(r,\theta)}{\partial r^2}+\frac{1}{r}\frac{\partial w_i(r,\theta)}{\partial r}=0. \tag{22}$$

According to Eq. (22), the solution of $w_i(r,\theta)$ can be given by

$$w_i(r,\theta)=\left(a_1^i+\ln r a_2^i\right)+\sum_{m=1}^{\infty}\left(r^m a_3^i+r^{-m}a_4^i\right)\cos(m\theta)+\sum_{m=1}^{\infty}\left(r^m a_5^i+r^{-m}a_6^i\right)\sin(m\theta), \tag{23}$$

where a_1^i, a_2^i, a_3^i, a_4^i, a_5^i and a_6^i are the coefficients determined from boundary conditions.

3.1.2 Case 2: n>0

When n>0, expressions of temperature (4) and displacement (20) are substituted into Eq. (18). The solutions of $u_i(r,\theta,z)$, $v_i(r,\theta,z)$ and $w_i(r,\theta,z)$ are derived out as:

$$\begin{aligned}
u_i(r,\theta,z)=&\sum_{n=1}^{\infty}\left(\sum_{g=1}^{4}a_{0g}^i e^{s_{0g}^i r}\right)\sin\frac{n\pi z}{l}+\sum_{m=1}^{\infty}\sum_{n=1}^{\infty}\left(\sum_{g=1}^{6}a_{1g}^i e^{s_{1g}^i r}\right)\cos(m\theta)\sin\frac{n\pi z}{l}\\
&+\sum_{m=1}^{\infty}\sum_{n=1}^{\infty}\left(\sum_{g=1}^{6}a_{2g}^i e^{s_{2g}^i r}\right)\sin(m\theta)\sin\frac{n\pi z}{l},\\
v_i(r,\theta,z)=&\sum_{n=1}^{\infty}\left(a_{05}^i e^{s_{05}^i r}+a_{06}^i e^{s_{06}^i r}\right)\sin\frac{n\pi z}{l}+\sum_{m=1}^{\infty}\sum_{n=1}^{\infty}\left(\sum_{g=1}^{6}\delta_{1g}^i a_{1g}^i e^{s_{1g}^i r}\right)\sin(m\theta)\sin\frac{n\pi z}{l}\\
&+\sum_{m=1}^{\infty}\sum_{n=1}^{\infty}\left(\sum_{g=1}^{6}\delta_{2g}^i a_{2g}^i e^{s_{2g}^i r}\right)\cos(m\theta)\sin\frac{n\pi z}{l},\\
w_i(r,\theta,z)=&\sum_{n=1}^{\infty}\left[\sum_{g=1}^{4}\zeta_{0g}^i a_{0g}^i e^{s_{0g}^i r}-\frac{(3\lambda_i+2G_i)\alpha_i l}{(\lambda_i+G_i)n\pi}e^{\alpha_n^i r}H_{ni}^1-\frac{(3\lambda_i+2G_i)\alpha_i l}{(\lambda_i+G_i)n\pi}e^{\beta_n^i r}H_{ni}^2\right]\cos\frac{n\pi z}{l}\\
&+\sum_{m=1}^{\infty}\sum_{n=1}^{\infty}\left[\sum_{g=1}^{6}\zeta_{1g}^i a_{1g}^i e^{s_{1g}^i r}-\frac{(3\lambda_i+2G_i)\alpha_i l}{(\lambda_i+G_i)n\pi}e^{\alpha_{mn}^i r}H_{mni}^3-\frac{(3\lambda_i+2G_i)\alpha_i l}{(\lambda_i+G_i)n\pi}e^{\beta_{mn}^i r}H_{mni}^4\right]\cos(m\theta)\cos\frac{n\pi z}{l}\\
&+\sum_{m=1}^{\infty}\sum_{n=1}^{\infty}\left[\sum_{g=1}^{6}\zeta_{2g}^i a_{2g}^i e^{s_{2g}^i r}-\frac{(3\lambda_i+2G_i)\alpha_i l}{(\lambda_i+G_i)n\pi}e^{\alpha_{mn}^i r}H_{mni}^5-\frac{(3\lambda_i+2G_i)\alpha_i l}{(\lambda_i+G_i)n\pi}e^{\beta_{mn}^i r}H_{mni}^6\right]\sin(m\theta)\cos\frac{n\pi z}{l},
\end{aligned} \tag{24}$$

where a_{0g}^i, a_{1g}^i and a_{2g}^i (i=1, 2…N, g=1, 2,.., 6) are unknown coefficients which depend on the boundary conditions of ith shelled layer. Three sets of coefficients s_{0g}^i, ζ_{0g}^i, s_{1g}^i, ζ_{1g}^i, δ_{1g}^i and s_{2g}^i, ζ_{2g}^i, δ_{2g}^i can be determined from the derivation process of the formulas (24).

The first group of coefficients s_{0g}^i and ζ_{0g}^i (g=1, 2, 3, 4) can be obtained:

$$\zeta_{0g}^{i}=-\frac{\left(\lambda_i+G_i\right)\frac{n\pi}{l}\left(s_{0g}^{i}+\frac{1}{r_{i0}}\right)}{\left[G_i\left(s_{0g}^{i}\right)^2+\frac{G_i}{r_{i0}}s_{0g}^{i}-\left(\lambda_i+2G_i\right)\frac{n^2\pi^2}{l^2}\right]} \tag{25}$$

where, s_{0g}^{i} are the results of the equation:

$$\left(\lambda_i+2G_i\right)\left(s_{0g}^{i}\right)^4+\frac{2\left(\lambda_i+2G_i\right)}{r_{i0}}\left(s_{0g}^{i}\right)^3+\left[\frac{\lambda_i}{r_{i0}^2}-\left(\lambda_i+2G_i\right)\frac{2n^2\pi^2}{l^2}\right]\left(s_{0g}^{i}\right)^2$$
$$-\frac{2}{r_{i0}}\left[\frac{G_i}{r_{i0}^2}+\left(\lambda_i+2G_i\right)\frac{n^2\pi^2}{l^2}\right]\left(s_{0g}^{i}\right)+\left(\lambda_i+2G_i\right)\left(\frac{2}{r_{i0}^2}+\frac{n^2\pi^2}{l^2}\right)\frac{n^2\pi^2}{l^2}=0 \tag{26}$$

and

$$s_{05}^{i}=\frac{\sqrt{\frac{4n^2\pi^2r_{i0}^2}{l^2}+9}-1}{2r_{i0}},\quad s_{06}^{i}=\frac{-\sqrt{\frac{4n^2\pi^2r_{i0}^2}{l^2}+9}-1}{2r_{i0}}. \tag{27}$$

The second group of coefficients s_{1g}^{i}, ζ_{1g}^{i} and δ_{1g}^{i} (g=1, 2, 3, 4, 5, 6) can be obtained. s_{1g}^{i} is the roots of the following equation,

$$A_{11}^{ij}C_{13}^{ij}\left(\frac{m}{r_{i0}s_{1g}^{i}}B_{13}^{ij}-B_{12}^{ij}\right)+C_{11}^{ij}\left(A_{13}^{ij}B_{12}^{ij}-A_{12}^{ij}B_{13}^{ij}\right)+\frac{m}{r_{i0}s_{1g}^{i}}C_{13}^{ij}C_{13}^{ij}\left(\frac{m}{r_{i0}s_{1g}^{i}}A_{13}^{ij}-A_{12}^{ij}\right)=0 \tag{28}$$

and

$$\delta_{1g}^{i}=\frac{A_{11}^{ig}C_{12}^{ig}-A_{12}^{ig}C_{11}^{ig}}{B_{12}^{ig}C_{11}^{ig}-B_{11}^{ig}C_{12}^{ig}},\quad \zeta_{1g}^{i}=\frac{A_{11}^{ig}B_{12}^{ig}-A_{12}^{ig}B_{11}^{ig}}{B_{11}^{ig}C_{12}^{ig}-B_{12}^{ig}C_{11}^{ig}} \tag{29}$$

where,

$$A_{11}^{ig}=\left(\lambda_i+G_i\right)\frac{n\pi}{l}\left(s_{1g}^{i}+\frac{1}{r_{i0}}\right),\quad B_{11}^{ig}=\left(\lambda_i+G_i\right)\frac{mn\pi}{r_{i0}l},\quad B_{13}^{ig}=\left(\lambda_i+G_i\right)\frac{m}{r_{i0}}s_{1g}^{i}-\frac{3G_im}{r_{i0}^2},$$
$$C_{11}^{ig}=G_i\left(s_{1g}^{i}\right)^2+\frac{G_i}{r_{i0}}s_{1g}^{i}-\left[\left(\lambda_i+2G_i\right)\frac{n^2\pi^2}{l^2}+\frac{G_im^2}{r_{i0}^2}\right],\quad A_{12}^{ig}=\left(\lambda_i+G_i\right)\frac{m}{r_{i0}}s_{1g}^{i}+\left(\lambda_i+4G_i\right)\frac{m}{r_{i0}^2},$$
$$A_{13}^{ig}=\left(\lambda_i+2G_i\right)\left(s_{1g}^{i}\right)^2+\frac{\left(\lambda_i+2G_i\right)}{r_{i0}}s_{1g}^{i}-\left(\frac{n^2\pi^2G_i}{l^2}+\frac{m^2G_i}{r_{i0}^2}+\frac{2G_i}{r_{i0}^2}\right),\quad C_{13}^{ij}=-\left(\lambda_i+G_i\right)\frac{n\pi}{l}s_{1j}^{i},$$
$$B_{12}^{ig}=-\left\{G_i\left(s_{1g}^{i}\right)^2+\frac{G_i}{r_{i0}}s_{1g}^{i}-\left[\left(\lambda_i+2G_i\right)\frac{m^2}{r_{i0}^2}+G_i\frac{n^2\pi^2}{l^2}+\frac{2G_i}{r_{i0}^2}\right]\right\},\quad C_{12}^{ig}=-\left(\lambda_i+G_i\right)\frac{mn\pi}{r_{i0}l}. \tag{30}$$

The third group of coefficients s_{2g}^{i}, ζ_{2g}^{i} and δ_{2g}^{i} can be obtained. s_{2g}^{i} is the roots of the following equation,

$$A_{21}^{ig}C_{23}^{ig}\left(\frac{m}{r_{i0}s_{2g}^{i}}B_{23}^{ig}-B_{22}^{ig}\right)+C_{21}^{ig}\left(A_{23}^{ig}B_{22}^{ig}-A_{22}^{ig}B_{23}^{ig}\right)-\frac{m}{r_{i0}s_{2g}^{i}}C_{23}^{ig}C_{23}^{ig}\left(\frac{m}{r_{i0}s_{2g}^{i}}A_{23}^{ig}-A_{22}^{ig}\right)=0 \tag{31}$$

and

$$\delta_{2g}^{i}=\frac{A_{21}^{ig}C_{22}^{ig}-A_{22}^{ig}C_{21}^{ig}}{B_{22}^{ig}C_{21}^{ig}-B_{21}^{ig}C_{22}^{ig}},\qquad \zeta_{2g}^{i}=\frac{A_{21}^{ig}B_{22}^{ig}-A_{22}^{ig}B_{21}^{ig}}{B_{21}^{ig}C_{22}^{ig}-B_{22}^{ig}C_{21}^{ig}}, \tag{32}$$

where,

$$A_{21}^{ig}=\left(\lambda_i+G_i\right)\frac{n\pi}{l}\left(s_{2g}^{i}+\frac{1}{r_{i0}}\right),\quad B_{21}^{ig}=-\left(\lambda_i+G_i\right)\frac{mn\pi}{r_{i0}l},\ B_{23}^{ig}=-\left(\lambda_i+G_i\right)\frac{m}{r_{i0}}s_{2g}^{i}+\frac{3G_im}{r_{i0}^{2}},$$

$$C_{21}^{ig}=G_i\left(s_{2g}^{i}\right)^{2}+\frac{G_i}{r_{i0}}s_{2g}^{i}-\left[\left(\lambda_i+2G_i\right)\frac{n^{2}\pi^{2}}{l^{2}}+\frac{G_im^{2}}{r_{i0}^{2}}\right],\ A_{22}^{ig}=\left(\lambda_i+G_i\right)\frac{m}{r_{i0}}s_{2g}^{i}+\left(\lambda_i+4G_i\right)\frac{m}{r_{i0}^{2}},$$

$$A_{23}^{ig}=\left(\lambda_i+2G_i\right)\left(s_{2g}^{i}\right)^{2}+\frac{\left(\lambda_i+2G_i\right)}{r_{i0}}s_{2g}^{i}-\left(\frac{n^{2}\pi^{2}G_i}{l^{2}}+\frac{m^{2}G_i}{r_{i0}^{2}}+\frac{2G_i}{r_{i0}^{2}}\right),\ C_{23}^{ig}=-\left(\lambda_i+G_i\right)\frac{n\pi}{l}s_{2g}^{i},$$

$$B_{22}^{ig}=G_i\left(s_{2g}^{i}\right)^{2}+\frac{G_i}{r_{i0}}s_{2g}^{i}-\left[\left(\lambda_i+2G_i\right)\frac{m^{2}}{r_{i0}^{2}}+G_i\frac{n^{2}\pi^{2}}{l^{2}}+\frac{2G_i}{r_{i0}^{2}}\right],\ C_{22}^{ig}=-\left(\lambda_i+G_i\right)\frac{mn\pi}{r_{i0}l}. \tag{33}$$

As $w_i\left(r,\theta,z\right)\neq 0$ for n=0, the complete solutions for displacements are the combining Eqs. (23) and (24)

3.2 Stresses in a single layer

Take the solutions of displacement to equation (15), the complete stress components are given by

$$\begin{aligned}\sigma_r^{i}\left(r,\theta,z\right)=&\sum_{n=1}^{\infty}\sin\frac{n\pi z}{l}\left\{\sum_{g=1}^{4}a_{0g}^{i}e^{s_{0g}^{i}r}\left[\left(\lambda_i+2G_i\right)S_{0g}^{i}+\frac{\lambda_i}{r_{i0}}-\frac{n\pi\lambda_i}{l}\zeta_{0g}^{i}\right]\right.\\&\left.-\frac{\left(3\lambda_i+2G_i\right)}{\left(\lambda_i+G_i\right)}G_i\alpha_ie^{\alpha_n^{i}r}H_{ni}^{1}-\frac{\left(3\lambda_i+2G_i\right)}{\left(\lambda_i+G_i\right)}G_i\alpha_ie^{\beta_n^{i}r}H_{ni}^{2}\right\}\\&+\sum_{m=1}^{\infty}\sum_{n=1}^{\infty}\cos m\theta\sin\frac{n\pi z}{l}\left\{\sum_{g=1}^{6}a_{1g}^{i}e^{s_{1g}^{i}r}\left[\left(\lambda_i+2G_i\right)S_{1g}^{i}+\frac{m\lambda_i}{r_{i0}}\delta_{1g}^{i}+\frac{\lambda_i}{r_{i0}}-\frac{n\pi\lambda_i}{l}\zeta_{1g}^{i}\right]\right.\\&\left.-\frac{\left(3\lambda_i+2G_i\right)}{\left(\lambda_i+G_i\right)}G_i\alpha_ie^{\alpha_{mn}^{i}r}H_{mni}^{3}-\frac{\left(3\lambda_i+2G_i\right)}{\left(\lambda_i+G_i\right)}G_i\alpha_ie^{\beta_{mn}^{i}r}H_{mni}^{4}\right\}\\&+\sum_{m=1}^{\infty}\sum_{n=1}^{\infty}\sin m\theta\sin\frac{n\pi z}{l}\left\{\sum_{g=1}^{6}a_{2g}^{i}e^{s_{2g}^{i}r}\left[\left(\lambda_i+2G_i\right)S_{2g}^{i}-\frac{m\lambda_i}{r_{i0}}\delta_{2g}^{i}+\frac{\lambda_i}{r_{i0}}-\frac{n\pi\lambda_i}{l}\zeta_{2g}^{i}\right]\right.\\&\left.-\frac{\left(3\lambda_i+2G_i\right)}{\left(\lambda_i+G_i\right)}G_i\alpha_ie^{\alpha_{mn}^{i}r}H_{mni}^{5}-\frac{\left(3\lambda_i+2G_i\right)}{\left(\lambda_i+G_i\right)}G_i\alpha_ie^{\beta_{mn}^{i}r}H_{mni}^{6}\right\},\end{aligned}$$

$$\sigma_\theta^i(r,\theta,z)=\sum_{n=1}^{\infty}\sin\frac{n\pi z}{l}\left\{\sum_{g=1}^{4}a_{0g}^i e^{s_{0g}^i r}[\lambda_i S_{0g}^i+\frac{(\lambda_i+2G_i)}{r_{i0}}-\frac{n\pi\lambda_i}{l}\zeta_{0g}^i]\right.$$
$$\left.-\frac{(3\lambda_i+2G_i)}{(\lambda_i+G_i)}G_i\alpha_i e^{\alpha_n^i r}H_{ni}^1-\frac{(3\lambda_i+2G_i)}{(\lambda_i+G_i)}G_i\alpha_i e^{\beta_n^i r}H_{ni}^2\right\}$$
$$+\sum_{m=1}^{\infty}\sum_{n=1}^{\infty}\cos m\theta\sin\frac{n\pi z}{l}\left\{\sum_{g=1}^{6}a_{1g}^i e^{s_{1g}^i r}[\lambda_i S_{1g}^i+(\lambda_i+2G_i)\frac{m}{r_{i0}}\delta_{1g}^i+\frac{(\lambda_i+2G_i)}{r_{i0}}-\frac{n\pi\lambda_i}{l}\zeta_{1g}^i]\right.$$
$$\left.-\frac{(3\lambda_i+2G_i)}{(\lambda_i+G_i)}G_i\alpha_i e^{\alpha_{mn}^i r}H_{mni}^3-\frac{(3\lambda_i+2G_i)}{(\lambda_i+G_i)}G_i\alpha_i e^{\beta_{mn}^i r}H_{mni}^4\right\}$$
$$+\sum_{m=1}^{\infty}\sum_{n=1}^{\infty}\sin m\theta\sin\frac{n\pi z}{l}\left\{\sum_{g=1}^{6}a_{2g}^i e^{s_{2g}^i r}[\lambda_i S_{2g}^i-(\lambda_i+2G_i)\frac{m}{r_{i0}}\delta_{2g}^i+\frac{(\lambda_i+2G_i)}{r_{i0}}-\frac{n\pi\lambda_i}{l}\zeta_{2g}^i]\right.$$
$$\left.-\frac{(3\lambda_i+2G_i)}{(\lambda_i+G_i)}G_i\alpha_i e^{\alpha_{mn}^i r}H_{mni}^5-\frac{(3\lambda_i+2G_i)}{(\lambda_i+G_i)}G_i\alpha_i e^{\beta_{mn}^i r}H_{mni}^6\right\},$$

$$\sigma_z^i(r,\theta,z)=\sum_{n=1}^{\infty}\sin\frac{n\pi z}{l}\left\{\sum_{g=1}^{4}a_{0g}^i e^{s_{0g}^i r}[\lambda_i S_{0g}^i+\frac{\lambda_i}{r_{i0}}-(\lambda_i+2G_i)\frac{n\pi}{l}\zeta_{0g}^i]\right.$$
$$\left.+\frac{(3\lambda_i+2G_i)}{(\lambda_i+G_i)}G_i\alpha_i e^{\alpha_n^i r}H_{ni}^1+\frac{(3\lambda_i+2G_i)}{(\lambda_i+G_i)}G_i\alpha_i e^{\beta_n^i r}H_{ni}^2\right\}$$
$$+\sum_{m=1}^{\infty}\sum_{n=1}^{\infty}\cos m\theta\sin\frac{n\pi z}{l}\left\{\sum_{g=1}^{6}a_{1g}^i e^{s_{1g}^i r}[\lambda_i S_{1g}^i+\frac{m\lambda_i}{r_{i0}}\delta_{1g}^i-(\lambda_i+2G_i)\frac{n\pi}{l}\zeta_{1g}^i+\frac{\lambda_i}{r_{i0}}]\right.$$
$$\left.+\frac{(3\lambda_i+2G_i)}{(\lambda_i+G_i)}G_i\alpha_i e^{\alpha_{mn}^i r}H_{mni}^3+\frac{(3\lambda_i+2G_i)}{(\lambda_i+G_i)}G_i\alpha_i e^{\beta_{mn}^i r}H_{mni}^4\right\}$$
$$+\sum_{m=1}^{\infty}\sum_{n=1}^{\infty}\sin m\theta\sin\frac{n\pi z}{l}\left\{\sum_{g=1}^{6}a_{2g}^i e^{s_{2g}^i r}[\lambda_i S_{2g}^i-\frac{m\lambda_i}{r_{i0}}\delta_{2g}^i-(\lambda_i+2G_i)\frac{n\pi}{l}\zeta_{2g}^i+\frac{\lambda_i}{r_{i0}}]\right.$$
$$\left.+\frac{(3\lambda_i+2G_i)}{(\lambda_i+G_i)}G_i\alpha_i e^{\alpha_{mn}^i r}H_{mni}^5+\frac{(3\lambda_i+2G_i)}{(\lambda_i+G_i)}G_i\alpha_i e^{\beta_{mn}^i r}H_{mni}^6\right\},$$

$$\tau_{\theta z}^i(r,\theta,z)=mG_i\left[\sum_{m=1}^{\infty}(-1)\left(r^{m-1}a_3^i+r^{-m-1}a_4^i\right)\sin m\theta+\sum_{m=1}^{\infty}\left(r^{m-1}a_5^i+r^{-m-1}a_6^i\right)\cos m\theta\right]$$
$$+\sum_{n=1}^{\infty}\cos\frac{n\pi z}{l}\left[\frac{n\pi G_i}{l}\left(a_{05}^i e^{s_{05}^i r}+a_{06}^i e^{s_{06}^i r}\right)\right]$$
$$+\sum_{m=1}^{\infty}\sum_{n=1}^{\infty}\sin m\theta\cos\frac{n\pi z}{l}\left[\sum_{g=1}^{6}G_i a_{1g}^i e^{s_{1g}^i r}\left(\frac{n\pi}{l}\delta_{1g}^i-\frac{m}{r_{i0}}\zeta_{1g}^i\right)\right.$$
$$\left.+\frac{(3\lambda_i+2G_i)}{(\lambda_i+G_i)}\frac{mG_i\alpha_i l}{n\pi r_{i0}}e^{\alpha_{mn}^i r}H_{mni}^3+\frac{(3\lambda_i+2G_i)}{(\lambda_i+G_i)}\frac{mG_i\alpha_i l}{n\pi r_{i0}}e^{\beta_{mn}^i r}H_{mni}^4\right]$$
$$+\sum_{m=1}^{\infty}\sum_{n=1}^{\infty}\cos m\theta\cos\frac{n\pi z}{l}\left[\sum_{g=1}^{6}G_i a_{2g}^i e^{s_{2g}^i r}\left(\frac{n\pi}{l}\delta_{2g}^i+\frac{m}{r_{i0}}\zeta_{2g}^i\right)\right.$$
$$\left.-\frac{(3\lambda_i+2G_i)}{(\lambda_i+G_i)}\frac{mG_i\alpha_i l}{n\pi r_{i0}}e^{\alpha_{mn}^i r}H_{mni}^5-\frac{(3\lambda_i+2G_i)}{(\lambda_i+G_i)}\frac{mG_i\alpha_i l}{n\pi r_{i0}}e^{\beta_{mn}^i r}H_{mni}^6\right],$$

$$
\begin{aligned}
\tau_{rz}^{i}\left(r,\theta,z\right)=&G_i\left[\frac{a_2^i}{r}+\sum_{m=1}^{\infty}\left(mr^{m-1}a_3^i-mr^{-m-1}a_4^i\right)\cos m\theta+\sum_{m=1}^{\infty}\left(mr^{m-1}a_5^i-mr^{-m-1}a_6^i\right)\sin m\theta\right]\\
&+\sum_{n=1}^{\infty}\cos\frac{n\pi z}{l}\left[\sum_{g=1}^{4}G_i a_{0g}^i e^{s_{0g}^i r}\left(\frac{n\pi}{l}+\zeta_{0g}^i S_{0g}^i\right)\right.\\
&\left.-\frac{\left(3\lambda_i+2G_i\right)}{\left(\lambda_i+G_i\right)}\frac{G_i\alpha_i\alpha_n^i l}{n\pi}e^{\alpha_n^i r}H_{ni}^1-\frac{\left(3\lambda_i+2G_i\right)}{\left(\lambda_i+G_i\right)}\frac{G_i\alpha_i\beta_n^i l}{n\pi}e^{\beta_n^i r}H_{ni}^2\right]\\
&+\sum_{m=1}^{\infty}\sum_{n=1}^{\infty}\cos m\theta\cos\frac{n\pi z}{l}\left[\sum_{g=1}^{6}G_i a_{1g}^i e^{s_{1g}^i r}\left(\frac{n\pi}{l}+S_{1g}^i\zeta_{1g}^i\right)\right.\\
&\left.-\frac{\left(3\lambda_i+2G_i\right)}{\left(\lambda_i+G_i\right)}\frac{G_i\alpha_i\alpha_{mn}^i l}{n\pi}e^{\alpha_{mn}^i r}H_{mni}^3-\frac{\left(3\lambda_i+2G_i\right)}{\left(\lambda_i+G_i\right)}\frac{G_i\alpha_i\beta_{mn}^i l}{n\pi}e^{\beta_{mn}^i r}H_{mni}^4\right]\\
&+\sum_{m=1}^{\infty}\sum_{n=1}^{\infty}\sin m\theta\cos\frac{n\pi z}{l}\left[\sum_{g=1}^{6}G_i a_{2g}^i e^{s_{2g}^i r}\left(\frac{n\pi}{l}+S_{2g}^i\zeta_{2g}^i\right)\right.\\
&\left.-\frac{\left(3\lambda_i+2G_i\right)}{\left(\lambda_i+G_i\right)}\frac{G_i\alpha_i\alpha_{mn}^i l}{n\pi}e^{\alpha_{mn}^i r}H_{mni}^5-\frac{\left(3\lambda_i+2G_i\right)}{\left(\lambda_i+G_i\right)}\frac{G_i\alpha_i\beta_{mn}^i l}{n\pi}e^{\beta_{mn}^i r}H_{mni}^6\right],\\
\tau_{r\theta}^{i}\left(r,\theta,z\right)=&\sum_{n=1}^{\infty}\sin\frac{n\pi z}{l}\left[G_i a_{05}^i e^{s_{05}^i r}\left(s_{05}^i-\frac{1}{r_{i0}}\right)+G_i a_{06}^i e^{s_{06}^i r}\left(s_{06}^i-\frac{1}{r_{i0}}\right)\right]\\
&+\sum_{m=1}^{\infty}\sum_{n=1}^{\infty}\sin m\theta\sin\frac{n\pi z}{l}\left\{\sum_{g=1}^{6}G_i a_{1g}^i e^{s_{1g}^i r}\left[-\frac{m}{r_{i0}}+\left(S_{1g}^i-\frac{1}{r_{i0}}\right)\delta_{1g}^i\right]\right\}\\
&+\sum_{m=1}^{\infty}\sum_{n=1}^{\infty}\cos m\theta\sin\frac{n\pi z}{l}\left\{\sum_{g=1}^{6}G_i a_{2g}^i e^{s_{2g}^i r}\left[\frac{m}{r_{i0}}+\left(S_{2g}^i-\frac{1}{r_{i0}}\right)\delta_{2g}^i\right]\right\}.
\end{aligned}
\tag{34}
$$

3.3 Induction formulas of displacement and stress

The induction formulas are divided into two parts based on solutions of displacement and stress for case 1: n=0 and case 2: n>0.

3.3.1 Case 1: n=0

When n=0, the displacements and stresses as given in Eqs. (23) and (34) can be shortened as:

$$
\left[\varpi_m^i\left(r_i,\theta\right)\right]=\begin{bmatrix}w_i\left(r,\theta\right)\\ \tau_{rz}^i\left(r,\theta\right)\end{bmatrix}=\begin{bmatrix}W_0^i\left(r\right)\\ X_0^i\left(r\right)\end{bmatrix}+\sum_{m=1}^{\infty}\begin{bmatrix}W_{m1}^i\left(r\right)\cos m\theta\\ X_{m1}^i\left(r\right)\cos m\theta\end{bmatrix}+\sum_{m=1}^{\infty}\begin{bmatrix}W_{m2}^i\left(r\right)\sin m\theta\\ X_{m2}^i\left(r\right)\sin m\theta\end{bmatrix}
\tag{35}
$$

where $W_0^i\left(r\right)$, $W_{m1}^i\left(r\right)$ and $W_{m2}^i\left(r\right)$ are defined as the displacement functions, $X_0^i\left(r\right)$, $X_{m1}^i\left(r\right)$ and $X_{m2}^i\left(r\right)$ are stress functions.

For brevity, Eqs. (23), (34) and (35) can be rewritten as

$$
\left[R_0^i\left(r\right)\right]=\left[E_0^i\left(r\right)\right]\left[\Delta_0^i\right],\ \left[R_{m1}^i\left(r\right)\right]=\left[E_{m1}^i\left(r\right)\right]\left[\Delta_{m1}^i\right],\ \left[R_{m2}^i\left(r\right)\right]=\left[E_{m2}^i\left(r\right)\right]\left[\Delta_{m2}^i\right],
\tag{36}
$$

in which,

$$
\left[R_0^i\left(r\right)\right]=\begin{bmatrix}W_0^i\left(r\right)\\ X_0^i\left(r\right)\end{bmatrix},\quad \left[R_{m1}^i\left(r\right)\right]=\begin{bmatrix}W_{m1}^i\left(r\right)\\ X_{m1}^i\left(r\right)\end{bmatrix},\quad \left[R_{m2}^i\left(r\right)\right]=\begin{bmatrix}W_{m2}^i\left(r\right)\\ X_{m2}^i\left(r\right)\end{bmatrix},
$$

$$\left[E_0^i(r)\right]=\begin{bmatrix}1 & \ln r\\ 0 & \dfrac{G_i}{r}\end{bmatrix},\ \left[\Delta_0^i\right]=\begin{bmatrix}a_1^i\\ a_2^i\end{bmatrix},\ \left[E_{m1}^i(r)\right]=\begin{bmatrix}r^m & r^{-m}\\ G_i m r^{m-1} & -G_i m r^{-m-1}\end{bmatrix},\ \left[\Delta_{m1}^i\right]=\begin{bmatrix}a_3^i\\ a_4^i\end{bmatrix},$$

$$\left[E_{m2}^i(r)\right]=\begin{bmatrix}r^m & r^{-m}\\ G_i m r^{m-1} & -G_i m r^{-m-1}\end{bmatrix},\quad \left[\Delta_{m2}^i\right]=\begin{bmatrix}a_5^i\\ a_6^i\end{bmatrix}. \tag{37}$$

On basis of the continuities of physical quantities on the interface, we have

$$\left[\varpi_m^i(r_i,\theta)\right]=\left[\varpi_m^{i+1}(r_i,\theta)\right]. \tag{38}$$

Thus, the relationships of physical quantities between qth and the innermost layers are given by:

$$\left[R_0^q(r_q)\right]=\left\{\prod_{i=1}^{q}\left[E_0^i(r_i)\right]\left[E_0^i(r_{i-1})\right]^{-1}\right\}\left[R_0^1(r_0)\right],$$

$$\left[R_{m1}^q(r_q)\right]=\left\{\prod_{i=1}^{q}\left[E_{m1}^i(r_i)\right]\left[E_{m1}^i(r_{i-1})\right]^{-1}\right\}\left[R_{m1}^1(r_0)\right],$$

$$\left[R_{m2}^q(r_q)\right]=\left\{\prod_{i=1}^{q}\left[E_{m2}^i(r_i)\right]\left[E_{m2}^i(r_{i-1})\right]^{-1}\right\}\left[R_{m2}^1(r_0)\right]. \tag{39}$$

3.3.2 Case 2: n>0

When $n>0$, the displacements and stresses of an isotropic layer as given in Eqs. (28) and (39) can be shortly rewritten as:

$$\begin{bmatrix}u_i(r,\theta,z)\\ v_i(r,\theta,z)\\ w_i(r,\theta,z)\\ \sigma_r^i(r,\theta,z)\\ \tau_{rz}^i(r,\theta,z)\\ \tau_{r\theta}^i(r,\theta,z)\end{bmatrix}=\sum_{n=1}^{\infty}\begin{bmatrix}U_{n0}^i(r)\sin\dfrac{n\pi z}{l}\\ V_{n0}^i(r)\sin\dfrac{n\pi z}{l}\\ W_{n0}^i(r)\cos\dfrac{n\pi z}{l}\\ Z_{n0}^i(r)\sin\dfrac{n\pi z}{l}\\ X_{n0}^i(r)\cos\dfrac{n\pi z}{l}\\ Y_{n0}^i(r)\sin\dfrac{n\pi z}{l}\end{bmatrix}+\sum_{m=1}^{\infty}\sum_{n=1}^{\infty}\begin{bmatrix}U_{mn1}^i(r)\cos(m\theta)\sin\dfrac{n\pi z}{l}\\ V_{mn1}^i(r)\sin(m\theta)\sin\dfrac{n\pi z}{l}\\ W_{mn1}^i(r)\cos(m\theta)\cos\dfrac{n\pi z}{l}\\ Z_{mn1}^i(r)\cos m\theta\sin\dfrac{n\pi z}{l}\\ X_{mn1}^i(r)\cos m\theta\cos\dfrac{n\pi z}{l}\\ Y_{mn1}^i(r)\sin m\theta\sin\dfrac{n\pi z}{l}\end{bmatrix}+\sum_{m=1}^{\infty}\sum_{n=1}^{\infty}\begin{bmatrix}U_{mn2}^i(r)\sin(m\theta)\sin\dfrac{n\pi z}{l}\\ V_{mn2}^i(r)\cos(m\theta)\sin\dfrac{n\pi z}{l}\\ W_{mn2}^i(r)\sin(m\theta)\cos\dfrac{n\pi z}{l}\\ Z_{mn2}^i(r)\sin m\theta\sin\dfrac{n\pi z}{l}\\ X_{mn2}^i(r)\sin m\theta\cos\dfrac{n\pi z}{l}\\ Y_{mn2}^i(r)\cos m\theta\sin\dfrac{n\pi z}{l}\end{bmatrix}, \tag{40}$$

where $U_{n0}^i(r)$, $V_{n0}^i(r)$, $W_{n0}^i(r)$, $U_{mn1}^i(r)$, $V_{mn1}^i(r)$, $W_{mn1}^i(r)$, $U_{mn2}^i(r)$, $V_{mn2}^i(r)$ and $W_{mn2}^i(r)$ are displacement functions, $Z_{n0}^i(r)$, $X_{n0}^i(r)$, $Y_{n0}^i(r)$, $Z_{mn1}^i(r)$, $X_{mn1}^i(r)$, $Y_{mn1}^i(r)$, $Z_{mn2}^i(r)$, $X_{mn2}^i(r)$ and $Y_{mn2}^i(r)$ are stress functions.

For brevity, Eqs. (24), (34) and (40) can be expressed as

$$\left[R_{n0}^i(r)\right]=\left[E_{n0}^i(r)\right]\left[\Delta_{n0}^i\right]+\left[Q_{n0}^i(r)\right],\quad \left[R_{mn1}^i(r)\right]=\left[E_{mn1}^i(r)\right]\left[\Delta_{mn1}^i\right]+\left[Q_{mn1}^i(r)\right],$$

$$\left[R_{mn2}^i(r)\right]=\left[E_{mn2}^i(r)\right]\left[\Delta_{mn2}^i\right]+\left[Q_{mn2}^i(r)\right], \tag{41}$$

in which, $\left[R_{n0}^{i}(r)\right]$, $\left[R_{mn1}^{i}(r)\right]$, $\left[R_{mn2}^{i}(r)\right]$, $\left[E_{n0}^{i}(r)\right]$, $\left[\Delta_{n0}^{i}\right]$, $\left[Q_{n0}^{i}(r)\right]$, $\left[E_{mn1}^{i}(r)\right]$, $\left[\Delta_{mn1}^{i}\right]$, $\left[Q_{mn1}^{i}(r)\right]$, $\left[E_{mn2}^{i}(r)\right]$, $\left[\Delta_{mn2}^{i}\right]$ and $\left[Q_{mn2}^{i}(r)\right]$ are given in detail in Appendix A.

On basis of the compatibility of physical quantities at the interface, the relationships between qth (q=2, 3, …, N) and innermost layers are given by:

$$\begin{aligned}
\left[R_{n0}^{q}(r_q)\right] &= \left\{\prod_{i=1}^{q}\left[E_{n0}^{i}(r_i)\right]\left[E_{n0}^{i}(r_{i-1})\right]^{-1}\right\}\left[R_{n0}^{1}(r_0)\right] - \left\{\prod_{i=1}^{q}\left[E_{n0}^{i}(r_i)\right]\left[E_{n0}^{i}(r_{i-1})\right]^{-1}\right\}\left[Q_{n0}^{1}(r_0)\right] \\
&+ \sum_{g=2}^{q}\left\{\prod_{i=g}^{q}\left[E_{n0}^{i}(r_i)\right]\left[E_{n0}^{i}(r_{i-1})\right]^{-1}\right\}\left\{\left[Q_{n0}^{g-1}(r_{(g-1)})\right] - \left[Q_{n0}^{g}(r_{(g-1)})\right]\right\} + \left[Q_{n0}^{q}(r_q)\right], \\
\left[R_{mn1}^{q}(r_q)\right] &= \left\{\prod_{i=1}^{q}\left[E_{mn1}^{i}(r_i)\right]\left[E_{mn1}^{i}(r_{i-1})\right]^{-1}\right\}\left[R_{mn1}^{1}(r_0)\right] - \left\{\prod_{i=1}^{q}\left[E_{mn1}^{i}(r_i)\right]\left[E_{mn1}^{i}(r_{i-1})\right]^{-1}\right\}\left[Q_{mn1}^{1}(r_0)\right] \\
&+ \sum_{g=2}^{q}\left\{\prod_{i=g}^{q}\left[E_{mn1}^{i}(r_i)\right]\left[E_{mn1}^{i}(r_{i-1})\right]^{-1}\right\}\left\{\left[Q_{mn1}^{g-1}(r_{(g-1)})\right] - \left[Q_{mn1}^{g}(r_{(g-1)})\right]\right\} + \left[Q_{mn1}^{q}(r_q)\right], \\
\left[R_{mn2}^{q}(r_q)\right] &= \left\{\prod_{i=1}^{q}\left[E_{mn2}^{i}(r_i)\right]\left[E_{mn2}^{i}(r_{i-1})\right]^{-1}\right\}\left[R_{mn2}^{1}(r_0)\right] - \left\{\prod_{i=1}^{q}\left[E_{mn2}^{i}(r_i)\right]\left[E_{mn2}^{i}(r_{i-1})\right]^{-1}\right\}\left[Q_{mn2}^{1}(r_0)\right] \\
&+ \sum_{g=2}^{q}\left\{\prod_{i=g}^{q}\left[E_{mn2}^{i}(r_i)\right]\left[E_{mn2}^{i}(r_{i-1})\right]^{-1}\right\}\left\{\left[Q_{mn2}^{g-1}(r_{(g-1)})\right] - \left[Q_{mn2}^{g}(r_{(g-1)})\right]\right\} + \left[Q_{mn2}^{q}(r_q)\right].
\end{aligned} \tag{42}$$

3.4 Coefficients of displacement and stress

In this analysis, the mechanical loads are not considered. If existed, the superposition method is adopted. The temperature conditions of cylindrical shells are

$$\begin{aligned}
&\sigma_r^1(r_0,\theta,z) = \sigma_r^N(r_N,\theta,z) = 0,\ \tau_{r\theta}^1(r_0,\theta,z) = \tau_{r\theta}^N(r_N,\theta,z) = 0, \\
&\tau_{rz}^1(r_0,\theta,z) = \tau_{rz}^N(r_N,\theta,z) = 0.
\end{aligned} \tag{43}$$

The two cases n=0 and n>0 are identified and are considered separately.

3.4.1 Case 1: n=0

When n=0, substituting Eq. (43) into Eq. (39) (taking q=N), the relationships of physical quantities between outer and inner layers are given by

$$\begin{aligned}
\begin{bmatrix} W_0^N(r_N) \\ 0 \end{bmatrix} &= \left\{\prod_{i=1}^{N}\left[E_0^i(r_i)\right]\left[E_0^i(r_{i-1})\right]^{-1}\right\}\begin{bmatrix} W_0^1(r_0) \\ 0 \end{bmatrix}, \\
\begin{bmatrix} W_{m1}^N(r_N) \\ 0 \end{bmatrix} &= \left\{\prod_{i=1}^{N}\left[E_{m1}^i(r_i)\right]\left[E_{m1}^i(r_{i-1})\right]^{-1}\right\}\begin{bmatrix} W_{m1}^1(r_0) \\ 0 \end{bmatrix}, \\
\begin{bmatrix} W_{m2}^N(r_N) \\ 0 \end{bmatrix} &= \left\{\prod_{i=1}^{N}\left[E_{m2}^i(r_i)\right]\left[E_{m2}^i(r_{i-1})\right]^{-1}\right\}\begin{bmatrix} W_{m2}^1(r_0) \\ 0 \end{bmatrix}.
\end{aligned} \tag{44}$$

The displacement $W_0^1(r_0)$, $W_0^N(r_N)$, $W_{m1}^1(r_0)$, $W_{m1}^N(r_N)$, $W_{m2}^1(r_0)$ and $W_{m2}^N(r_N)$ can be determined from Eq. (44). The functions $\left[R_0^q(r_q)\right]$, $\left[R_{m1}^q(r_q)\right]$ and $\left[R_{m2}^q(r_q)\right]$ (q=2,3…N-1) are obtained from equation (39) and the unknown coefficients a_1^i, a_2^i, a_3^i, a_4^i, a_5^i and a_6^i (i=1, 2…N) are determined from Eq. (36).

3.4.2 Case 2: n>0

When n>0, substituting Eq. (43) into Eq. (42) (taking q=N), the relationships of physical quantities between Nth and innermost layers are

$$\begin{bmatrix} U_{n0}^N(r_N) \\ V_{n0}^N(r_N) \\ W_{n0}^N(r_N) \\ 0 \\ 0 \\ 0 \end{bmatrix} = \begin{bmatrix} \nabla_{n0}^{11} & \nabla_{n0}^{12} \\ \nabla_{n0}^{21} & \nabla_{n0}^{22} \end{bmatrix} \begin{bmatrix} U_{n0}^1(r_0) \\ V_{n0}^1(r_0) \\ W_{n0}^1(r_0) \\ 0 \\ 0 \\ 0 \end{bmatrix} + \begin{bmatrix} \Omega_{n0}^1 \\ \Omega_{n0}^2 \\ \Omega_{n0}^3 \\ \Omega_{n0}^4 \\ \Omega_{n0}^5 \\ \Omega_{n0}^6 \end{bmatrix}, \begin{bmatrix} U_{mn1}^N(r_N) \\ V_{mn1}^N(r_N) \\ W_{mn1}^N(r_N) \\ 0 \\ 0 \\ 0 \end{bmatrix} = \begin{bmatrix} \nabla_{mn1}^{11} & \nabla_{mn1}^{12} \\ \nabla_{mn1}^{21} & \nabla_{mn1}^{22} \end{bmatrix} \begin{bmatrix} U_{mn1}^1(r_0) \\ V_{mn1}^1(r_0) \\ W_{mn1}^1(r_0) \\ 0 \\ 0 \\ 0 \end{bmatrix} + \begin{bmatrix} \Omega_{mn1}^1 \\ \Omega_{mn1}^2 \\ \Omega_{mn1}^3 \\ \Omega_{mn1}^4 \\ \Omega_{mn1}^5 \\ \Omega_{mn1}^6 \end{bmatrix},$$

$$\begin{bmatrix} U_{mn2}^N(r_N) \\ V_{mn2}^N(r_N) \\ W_{mn2}^N(r_N) \\ 0 \\ 0 \\ 0 \end{bmatrix} = \begin{bmatrix} \nabla_{mn2}^{11} & \nabla_{mn2}^{12} \\ \nabla_{mn2}^{21} & \nabla_{mn2}^{22} \end{bmatrix} \begin{bmatrix} U_{mn2}^1(r_0) \\ V_{mn2}^1(r_0) \\ W_{mn2}^1(r_0) \\ 0 \\ 0 \\ 0 \end{bmatrix} + \begin{bmatrix} \Omega_{mn2}^1 \\ \Omega_{mn2}^2 \\ \Omega_{mn2}^3 \\ \Omega_{mn2}^4 \\ \Omega_{mn2}^5 \\ \Omega_{mn2}^6 \end{bmatrix}. \tag{45}$$

The detail of each matrix and abbreviations in Eq. (45) is given in Appendix B.

The coefficients $U_{n0}^1(r_0)$, $V_{n0}^1(r_0)$, $W_{n0}^1(r_0)$, $U_{n0}^N(r_N)$, $V_{n0}^N(r_N)$, $W_{n0}^N(r_N)$, $U_{mn1}^1(r_0)$, $V_{mn1}^1(r_0)$, $W_{mn1}^1(r_0)$, $U_{mn1}^N(r_N)$, $V_{mn1}^N(r_N)$, $W_{mn1}^N(r_N)$, $U_{mn2}^1(r_0)$, $V_{mn2}^1(r_0)$, $W_{mn2}^1(r_0)$, $U_{mn2}^N(r_N)$, $V_{mn2}^N(r_N)$ and $W_{mn2}^N(r_N)$ can be obtained through equation (45). The displacement and stress functions $\left[R_{n0}^q(r_q)\right]$, $\left[R_{mn1}^q(r_q)\right]$ and $\left[R_{mn2}^q(r_q)\right]$ (q=2,3…N-1) are obtained from equation (42) and a_{0g}^q, a_{1g}^q, a_{2g}^q (g=1, 2,…,6) can be obtained through equation (41). The complete displacement and stress distributions of the laminated shell are given by substituting a_g^i, a_{0g}^i, a_{1j}^i and a_{2g}^i respectively into Eqs. (23), (24) and (34).

4 Convergence and comparison

A numerical example has been implemented to investigate the convergence ability of the present method. The double precision computations are conducted in the following numerical calculations. As the most common laminated structure in engineering practice, a triple-layer cylindrical shell is present as instance. The materials of surface layers and middle layer are steel and concrete, respectively, and their radii are r_0=1.5 m, r_1=1.9 m, r_2=2.3 m, r_3=2.7 m. The shell length is l=10 m. Poisson's ratios of steel and concrete are 0.3 and 0.2, respectively. The thermal conductivities of steel and concrete are 50

W/(m·°C) and 2 W/(m·°C), respectively. The Young's Moduli of steel and concrete are 200GPa and 30GPa, respectively. Thermal expansion coefficients of steel and concrete are 1.2×10^{-5}/℃ and 0.7×10^{-5}/℃, respectively. The inner surface of the cylindrical shell undergoes a uniform steady-state thermal load: $t_1(\theta, z)$=0℃, meanwhile the outer surface undergoes the thermal load:

$$t_p(\theta,z)=\begin{cases}t_0 & 0\le\theta\le\pi\\ 0 & -\pi<\theta<0\end{cases} \tag{46}$$

where, t_0=100 °C.

The laminated shell is divided into 15 thin layers. Limiting indices m and n in the infinite series to L in Eqs. (6), (25), (26) and (36), we have approximate results of displacement and stress in terms of L. Five different numbers for L=15, 20, 25, 30, 35 have been checked in the series. Tab. 1 provides the numerical results at r=1.6 m, θ=1.8 rad, z=4.2 m and r=2.0 m, θ=1.28 rad, z=3.2 m, respectively. Tab. 1 reflects that the data converge rapidly with the growing numbers of term L. There is little difference between solutions for L=30 and 35. Thus, the terms' number of Fourier series is set as L=30 in the subsequent calculations.

Table 1: Investigation of convergence

Position	L	u(mm)	v(mm)	σ_θ(MPa)	σ_z(MPa)	$\tau_{r\theta}$(MPa)
r=1.6 m, θ=1.8 rad, z=4.2 m	15	6.54	-1.92	108	198	2.89
	20	7.28	-1.98	119	232	3.12
	25	9.84	-2.28	125	258	3.28
	30	10.8	-2.40	161	286	4.56
	35	10.8	-2.40	161	286	4.56
r=2.0 m, θ=1.28 rad, z=3.2 m	15	6.82	2.12	13.8	39.6	-5.46
	20	7.28	2.48	15.8	41.8	-5.88
	25	8.96	2.59	16.8	43.2	-6.66
	30	9.60	2.70	17.9	44.5	-6.72
	35	9.60	2.70	17.9	44.5	-6.72

To evaluate the errors in adopting the thin layer approach in Eq. (2), the three-layer shell has been further divided progressively into 6, 9, 12, 15 and 18 thin layers. Tab. 2 presents the numerical results for displacements and stresses at r=1.6m, θ=1.8 rad, z=4.2 m and r=2.0 m, θ=1.28 rad, z=3.2 m, respectively. It is clear that the data for N=15 and 18 have identical three significant figures. This means we can eliminate the error through enlarging the number of the thin layers (i.e., decreasing the thickness of thin layers). A finite element (FE) simulation with the help of ANSYS software (Element types: solid 90 for temperature analysis, solid 186 for structural analysis) has been implemented to assure the validity of the current method. The comparison of results at the five locations

is given in Tab. 3, which suggests that the FEM simulation results agree well with the analytical solutions.

Table 2: The influence of total thinning layer numbers

Position	N	u(mm)	v(mm)	σ_θ(MPa)	σ_z(MPa)	$\tau_{r\theta}$(MPa)
r=1.6 m, θ=1.8 rad, z=4.2 m	6	10.2	-2.12	148	262	4.32
	9	10.3	-2.23	153	281	4.53
	12	10.8	-2.40	159	285	4.58
	15	10.8	-2.40	161	286	4.56
	18	10.8	-2.40	161	286	4.56
r=2.0 m, θ=1.28 rad, z=3.2 m	6	9.52	2.53	15.9	41.5	-6.46
	9	9.58	2.59	16.8	43.8	-6.58
	12	9.60	2.68	17.6	44.3	-6.71
	15	9.60	2.70	17.9	44.5	-6.72
	18	9.60	2.70	17.9	44.5	-6.72

Table 3: Comparison studies towards current results and FE results

Displacements and stresses	Method	θ=1.8 rad, z=4.2 m				
		r=1.50 m	r=1.80 m	r=2.10 m	r=2.40 m	r=2.70 m
u(mm)	Current	10.9	10.7	10.9	11.3	11.6
	FE	10.7	10.6	10.8	11.1	11.4
v(mm)	Current	-2.40	-2.40	-2.40	-2.40	-2.40
	FE	-2.39	-2.40	-2.40	-2.40	-2.40
σ_θ(MPa)	Current	180	134	14.0	-105	-103
	FE	175	131	13.8	-103	-101
σ_z(MPa)	Current	275	309	46.0	104	142
	FE	272	306	45.7	103	139
$\tau_{r\theta}$(MPa)	Current	0	7.09	5.07	4.22	0
	FE	0	7.04	5.04	4.18	0

Numerical data are compared with the results from Ayoubi et al. [Ayoubi and Alibeigloo (2017)] to validate the present method. The hollow cylinder in reference is an isotropic-one-walled functionally graded materials cylindrical shell with the dimensions of r_0=0.95 m, r_p=1.05m, l=3 m. The surface temperatures are $t_1(\theta, z)$=200K and $t_p(\theta, z)$=0, respectively. The outer surface is metal (Ni) with the material properties k_m=90.5 W/(m·K), E_m=206 GPa and α_m=1.33×10^{-5}/K. The inner surface is ceramic (SiC) with the material properties k_c=65 W/(m·K), E_c=427 GPa and α_c=4.3×10^{-6}/K. The material properties of the cylinder follow the laws:

$$E(r)=E_c(\frac{r}{r_0})^{m_1},\quad \alpha(r)=\alpha_c(\frac{r}{r_0})^{m_2},\quad k(r)=k_c(\frac{r}{r_0})^{m_3}, \tag{47}$$

where, $m_1=\dfrac{\ln\dfrac{E_m}{E_c}}{\ln\dfrac{r_P}{r_0}}$, $m_2=\dfrac{\ln\dfrac{\alpha_m}{\alpha_c}}{\ln\dfrac{r_P}{r_0}}$, $m_3=\dfrac{\ln\dfrac{k_m}{k_c}}{\ln\dfrac{r_P}{r_0}}$.

The functionally graded cylinder is divided into ten layers and the nondimensional stress σ_r^* along the thickness at z=1.5 m can be obtained in Tab. 4. From comparison of the present results with the reference, good agreement is found.

Table 4: Comparison of radial stresses σ_r^* through the thickness with reference

$r/(r_P-r_0)$	0.1	0.3	0.5	0.7	0.9
present	-0.676	-1.37	-1.35	-0.890	-0.277
reference	-0.674	-1.35	-1.34	-0.889	-0.277

Note: radial stresses $\sigma_r^*=\sigma_r/(\alpha_0 T_i E^*)$, $\alpha_0=10^{-6}$/K, T_i=200K, E^*=1 GPa

5 Parameter studies

In this part, the discussion of temperature, displacement and stress mainly is focused on the influences of surface temperature t_0, geometric dimensions, the number of laminated layers and the material properties.

5.1 Influence of surface temperatures

The first model is a triple-layered cylindrical shell. The layer radii are r_0=1.5 m, r_1=1.9 m, r_2=2.3 m, r_3=2.7 m, respectively. The shell length is l=10 m. The material properties are identical with that shell shown in Section 4. The outer surface of the shell undergoes three different thermal loads t_0: 50°C, 100°C, 150°C in Eq. (46). The temperature of the inner surface is constant as 0°C.

Fig. 2 illustrates the temperature change along the r direction at θ=1.8 rad, z=4.2 m for various temperature fields. It follows that the temperature variation rate within the surface layers along the r direction are pretty small in Fig. 2. However, the temperature gradient within the middle layer is larger because the thermal conductivity of the surface layers in the cylindrical shell is much greater than that of the core layer. Fig. 3 reflects the distributions of u, v, σ_r and $\tau_{\theta z}$. We can find from Figs. 2 and 3 that the absolute values of all physical quantities increase with the increasing thermal loads t_0 from the outer surface. It is clear from Figs. 3(a) and 3(b) that the u and v vary slightly with r but increase with the increasing thermal load. Fig. 3(c) presents that σ_r is always positive. Moreover, we can see from Fig. 3(d) that $\tau_{\theta z}$ are of discontinuity on the interfaces, i.e., different $\tau_{\theta z}$ exist for distinct material properties on two sides in the shell.

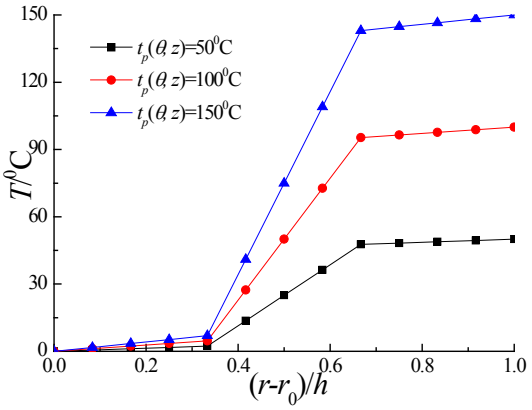

Figure 2: The temperature change along r-axis at θ=1.8 rad, z=4.2 m for a 3-layered cylindrical shell under different surface temperatures

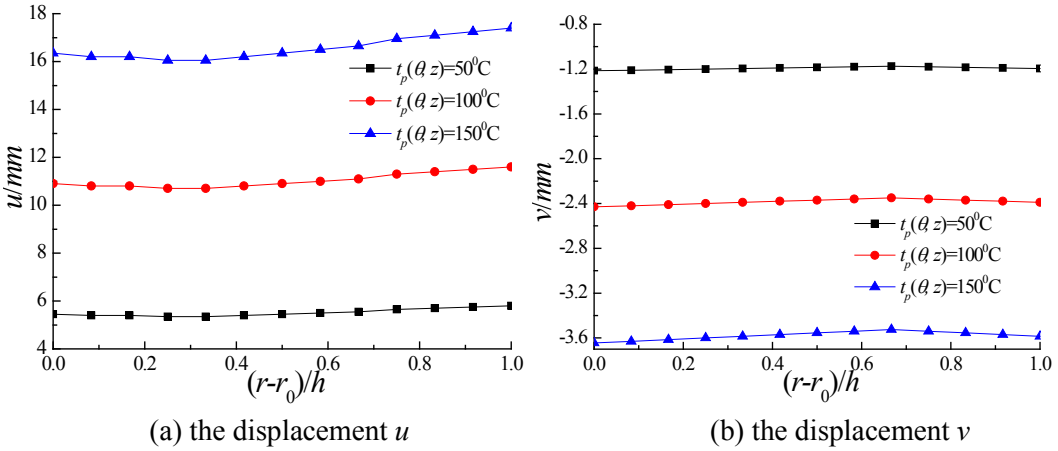

(a) the displacement u (b) the displacement v

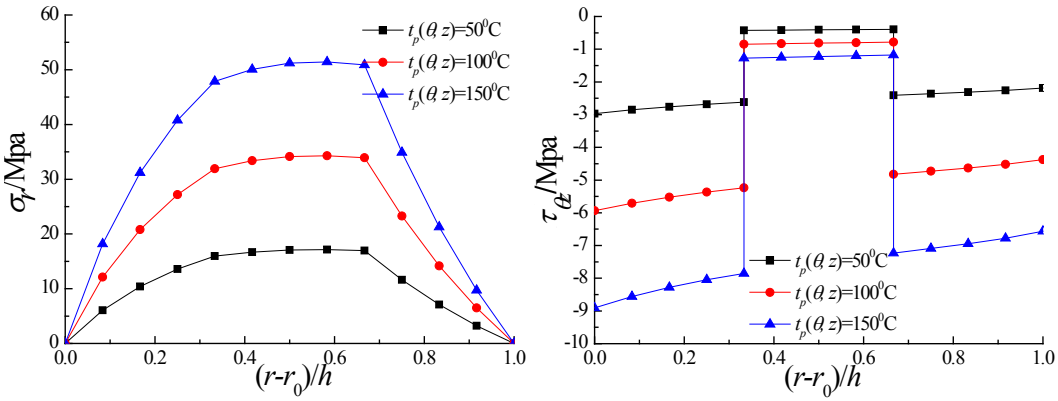

(c) the stress component σ_r (d) the stress component $\tau_{\theta z}$

Figure 3: Displacements and stresses at θ=1.8 rad, z=4.2 m under different thermal loads

To analyze the stress distribution features on the interface, the distributions of stresses σ_θ and $\tau_{\theta z}$ on two sides of the interface at r=1.9 m, z=4.25 m along the θ direction are depicted in Fig. 4 for t_0=100°C. Since the Young's modulus of steel is relatively greater, we can see that the absolute values of stresses in surface layers are greater than those in middle layer at all time.

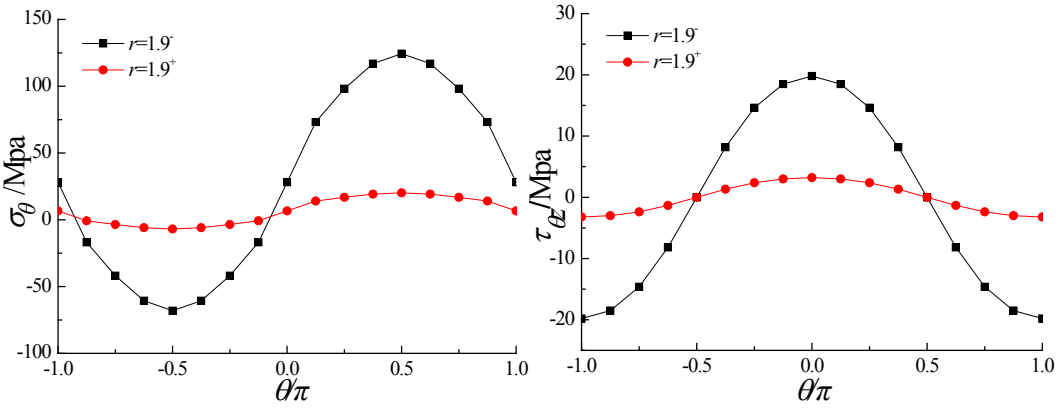

(a) stress σ_θ (b) stress $\tau_{\theta z}$

Figure 4: The σ_θ and $\tau_{\theta z}$ distribution for t_0=100°C at r=1.9 m, z=4.25 m

Note: the subscript "-" and superscript "+" indicate the position of inner and outer surfaces on the interface, respectively.

5.2 Figures influence of the ratio h/r_0

A three-layered cylindrical shell with thickness h (i.e., r_3-r_0)=1.2 m and h_1= h_2= h_3=0.4 m is studied in this part. We considered three different values r_0=1 m, 1.5 m and 3 m, for which h/r_0=1.20, 0.80 and 0.40 respectively. The shell length is l=10 m. The material properties of laminated shells are the same as given in Section 4. The outer surface in the cylindrical shell undergoes thermal load t_0=100°C in Eq. (46). The inner surface undergoes a constant thermal load $t_1(\theta, z)$=0°C.

The temperature distribution along the radial direction r at θ=1.8 rad, z=4.2 m is plotted in Fig. 5, and Fig. 6 presents the changes of u, v, σ_r and σ_z. Fig. 5 illustrates that the temperature distribution is almost constant with different ratio h/r_0. Figs. 6(a) and 6(b) reflect that absolute values for displacements u and v increase with increasing h/r_0. Fig. 6(c) tells that the change rates of σ_r and σ_z increase with the increasing h/r_0.

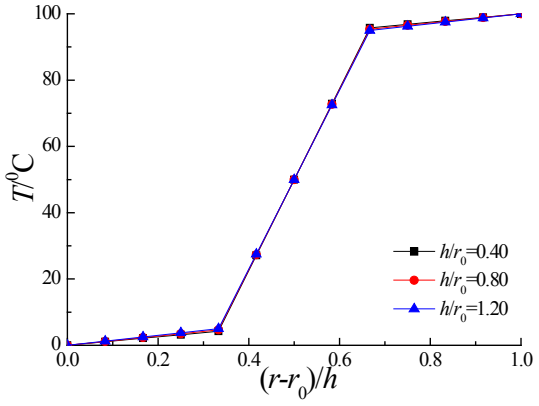

Figure 5: The temperature change at θ=1.8 rad, z=4.2 m along r-axis under different h/r_0

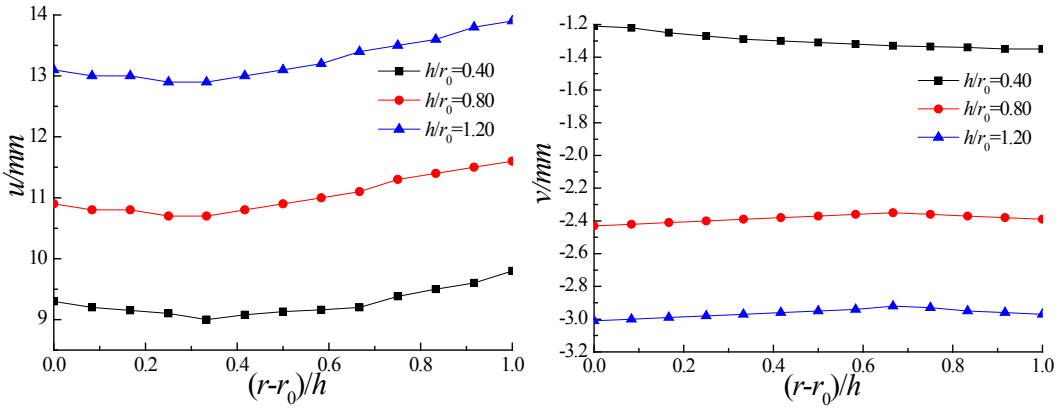

(a) the displacement u (b) the displacement v

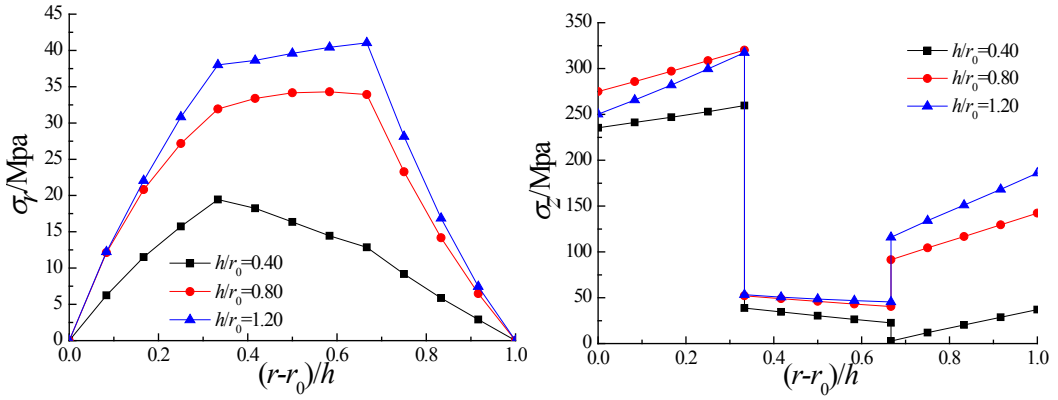

(c) the stress component σ_r (d) the stress component σ_z

Figure 6: Physical quantities at the r-axis at θ=1.8 rad, z=4.2 m under different h/r_0

5.3 Influence of material properties

The last model is to compare the displacement and the stress along the r-axis of three distinct two-layered shells. The material of the inner layer is steel, while the material of the outer layer is concrete. The inner dimension of the tube is r_0=2 m, and the outer dimension is r_2=3.2 m. Hence the thickness h of the tube equal to 1.2 m. All shells have the same length l=10 m. We considered three different thicknesses for the steel layer h_s=0.4 m, 0.6 m and 0.8 m for which h_s/h_c=2.0, 1.0 and 0.5 respectively. The outer surface in the layered shells undergoes a distributed thermal load with t_0=100°C in Eq. (46). The inner surface is suffered a constant temperature $t_1(\theta, z)$=20°C. The distributions of T, v, w, σ_z and τ_{rz} at $\theta=\pi/4$, z=4.5 m along the radial direction are given in Fig. 7 and Fig. 8. For cylindrical shells of the same total thickness, we can find temperature filed, thermal stresses and displacements are different. Fig. 7 reflects that the temperature T varies lightly in steel layer, as thermal conductivity of steel is greater than concrete. Figs. 8(a) and 8(b) clearly present that the displacement v and w change substantially in the shell of h_s=0.4 m. The reason is that the Young's modulus for steel is significantly greater than concrete. We can also observe from Fig. 8(c) that the change of σ_z on the interface between steel and concrete layers increases with decreasing ratio h_s/h_c. As shown in Fig. 8(d) τ_{rz} is almost invariant near the inner surface, however, τ_{rz} changes quite substantially in place away from the inner surface, say $(r-r_0)/h>0.2$.

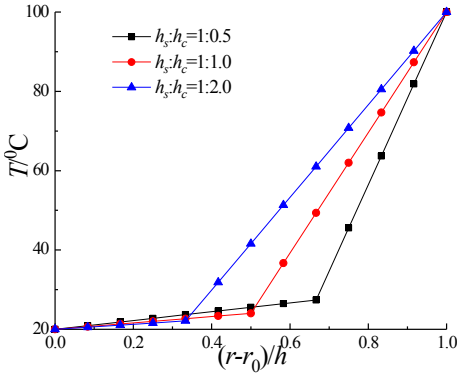

Figure 7: The temperature change at $\theta=\pi/4$ rad, z=4.5 m along r-axis to different laminates

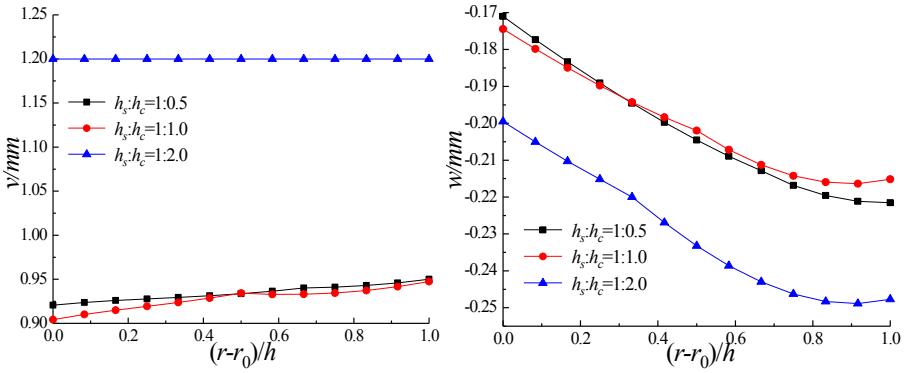

(a) the displacement v (b) the displacement w

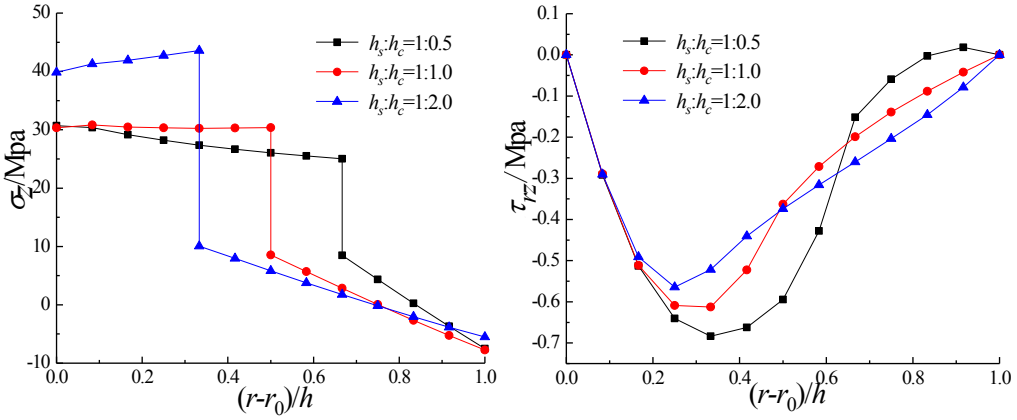

(c) the stress component σ_z (d) the stress component τ_{rz}

Figure 8: Displacement and stress distribution at $\theta=\pi/4$ rad, z=4.5 m along r-axis under different laminates

6 Conclusions

This study presents an investigation into simply-supported layered cylindrical shells subjected to thermal loads on the surface on basis of the theory of exact three-dimensional thermo-elasticity. With the consideration of the effect of transverse shear deformation and the continuities at the interface, the exact temperature and stress solutions can be readily derived by solving several sets of algebraic equations for laminated cylinders with arbitrary layers. Main conclusions are summarized as listed:

(1) By use of the theoretical method developed in this paper, the temperature distribution, displacement and stress of cylindrical layered shells under thermal loads can be derived in a straightforward way.

(2) A thinning layer approach is explored to solve the heat conduction equation and the three-dimensional thermo-elasticity equation. The results of FEM simulation are presented to compare with results due to the analytical method. The comparison of results suggests the accuracy and correctness of the present methodology. Also, the convergence property of the proposed method is examined and an excellent convergence property of the present approach is found. The present methodology can be used to study the thermal buckling problems.

(3) Results showed that the research objects in the shell consistently grow with the increasing thermal load on the outer surface. Stress σ_θ and $\tau_{\theta z}$ are of discontinuity on the interfaces, i.e., distinct material properties exist on two sides in the shell. The geometrical sizes and the material properties make significant influences on the temperature field, thermal stresses and displacements of layered cylindrical shells.

Acknowledgement: This work is financially supported by the Transportation Science and Technology Project of Jiangsu Province (Grant No. 2014Y01), the Seed Funding Program for Basic Research of the University of Hong Kong, the Research Foundation

for Advanced Talents of Jiangsu University (Grant No. 16JDG053) and the Basic Research Program of Jiangsu Province (Grant No. BK20160519, BK20160536).

References

Aziz, A.; Torabi, M. (2013): Thermal stresses in a hollow cylinder with convective boundary conditions on the inside and outside surfaces. *Journal of Thermal Stresses*, vol. 36, no. 10, pp. 1096-1111.

Ali, J. S. M.; Alsubari, S.; Aminanda, Y. (2016): Hygrothermoelastic analysis of orthotropic cylindrical shells. *Latin American Journal of Solids and Structures*, vol. 13, no. 3, pp. 573-589.

Ahmadi, I. (2017): A Galerkin layerwise formulation for three-dimensional stress analysis in long sandwich plates. *Steel and Composite Structures*, vol. 24, no. 5, pp. 523-536.

Alankaya, V.; Oktem, A. S. (2016): Static analysis of laminated and sandwich composite doubly-curved shallow shells. *Steel and Composite Structures*, vol. 20, no. 5, pp. 1043-1066.

Alankaya, V.; Erdonmez, C. (2017): Bending performance of laminated sandwich shells in hyperbolic paraboloidal form. *Steel and Composite Structures*, vol. 25, no. 3, pp. 337-346.

Akgöz, B.; Civalek, Ö. (2011): Nonlinear vibration analysis of laminated plates resting on nonlinear two-parameters elastic foundations. *Steel and Composite Structures*, vol. 11, no. 5, pp. 403-421.

Blanc, M.; Touratier, M. (2007): An efficient and simple refined model for temperature analysis in thin laminated composites. *Composite Structures*, vol. 77, no. 2, pp. 193-205.

Bishay, P. L.; Sladek, J.; Sladek, V.; Atluri, S. N. (2012): Analysis of functionally graded magneto-electro-elastic composite using hybrid/mixed finite elements and node-wise material properties. *Computers, Materials & Continua*, vol. 29, no. 3, pp. 213-261.

Baltacıoglu, A. K.; Akgöz, B.; Civalek, Ö. (2010): Nonlinear static response of laminated composite plates by discrete singular convolution method. *Composite Structures*, vol. 93, pp. 153-161.

Chang, Y. P.; Kang, C. S.; Chen, D. J. (1973): The use of fundamental green's functions for the solution of problems of heat conduction in anisotropic media. *International Journal of Heat and Mass Transfer*, vol. 16, no. 10, pp. 1905-1918.

Chen, X. L.; Liu, Y. J. (2001): Thermal stress analysis of multi-layer thin films and coatings by an advanced boundary element method. *Computer Modeling in Engineering & Sciences*, vol. 2, no. 3, pp. 337-349.

Civalek, Ö. (2007): Linear vibration analysis of isotropic conical shells by discrete singular convolution (DSC). *Structural Engineering and Mechanics*, vol. 25, no. 1, pp. 127-130.

Civalek, Ö. (2008): Vibration analysis of conical panels using the method of discrete singular convolution. *Communications in Numerical Methods in Engineering*, vol. 24, pp. 169-181.

Civalek, Ö. (2017): Free vibration of carbon nanotubes reinforced (CNTR) and

functionally graded shells and plates based on FSDT via discrete singular convolution method. *Composite Part B: Engineering*, vol. 111, pp. 45-59.

Civalek, Ö.; Acar, M. H. (2007): Discrete singular convolution method for the analysis of Mindlin plates on elastic foundations. *International Journal of Pressure Vessels and Piping*, vol, 84, no. 9, pp. 527-535.

Eason, G. (1962): Thermal stress in anisotropic cylinders. *Proceedings of the Edinburgh Mathematical Society*, vol. 13, no. 2, pp. 159-164.

Fard, K. M. (2015): Higher order static analysis of truncated conical sandwich panels with flexible cores. *Steel and Composite Structures*, vol. 19, no. 6, pp. 1333-1354.

Ghugal, Y. M.; Kulkarni, S. K. (2013): Thermal response of symmetric cross-ply laminated plates subjected to linear and non-linear thermo-mechanical loads. *Journal of Thermal Stresses*, vol. 36, no. 5, pp. 466-479.

Haji-Sheikh, A.; Beck, J. V.; Agonafer, D. (2003): Steady-state heat conduction in multi-layer bodies. *International Journal of Heat and Mass Transfer*, vol. 46, no. 13, pp. 2363-2379.

Hyer, M. W.; Cooper, D. E. (1986): Stresses and deformations in composite tubes due to circumferential temperature gradient. *Journal of Applied Mechanics*, vol. 53, no. 4, pp. 757-764.

Hyer, M. W.; Cooper, D. E.; Cohen, D. (1986): Stresses and deformations in cross-ply composite tubes subjected to a uniform temperature-change. *Journal of Thermal Stresses*, vol. 9, no. 2, pp. 97-117.

Hetnarski, R. B.; Ignaczak, J. (1993): Generalized thermoelasticity: closed-form solutions. *Journal of Thermal Stresses*, vol. 16, no. 4, pp. 473-498.

Huang, N. N.; Tauchert, T. R. (1992): Thermal stresses in doubly-curved cross-ply laminates. *International Journal of Solids and Structures*, vol. 29, no. 8, pp. 991-1000.

Heydarpour, Y.; Malekzadeh, P. (2019): Thermoelastic analysis of multilayered FG spherical shells based on Lord-Shulman theory. *Iranian Journal of Science and Technology-Transactions of Mechanical Engineering*, vol. 43, pp. 845-867.

Heydarpour, Y.; Malekzadeh, P.; Gholipour, F. (2019): Thermoelastic analysis of FG-GPLRC spherical shells under thermo-mechanical loadings based on Lord-Shulman theory. *Composite Part B: Engineering*, vol. 164, pp. 400-424.

Heydarpour, Y.; Malekzadeh, P.; Haghighi, M. R. G.; Vaghefi, M. (2012): Thermoelastic analysis of rotating laminated functionally graded cylindrical shells using layerwise differential quadrature method. *Acta Mechanica*, vol. 223, pp. 81-93.

Ieşan, D. (1980): Thermal stresses in composite cylinders. *Journal of Thermal Stresses*, vol. 3, no. 4, pp. 495-508.

Javaheri, R.; Eslami, M. R. (2002): Thermal buckling of functionally graded plates based on higher order theory. *Journal of Thermal Stresses*, vol. 25, no. 7, pp. 603-625.

Kumar, A.; Chakrabarti, A.; Ketkar, M. (2013): Analysis of laminated composite skew shells using higher order shear deformation theory. *Latin American Journal of Solids and Structures*, vol. 10, no. 5, pp. 391-419.

Kayhani, M. H.; Norouzi, M.; Delouei, A. A. (2012): A general analytical solution for heat conduction in cylindrical multilayer composite laminates. *International Journal of Thermal Sciences*, vol. 52, pp. 73-82.

Kayhani, M. H.; Shariati, M.; Nourozi, M.; Demneh, M. K. (2009). Exact solution of conductive heat transfer in cylindrical composite laminate. *Heat and Mass Transfer*, vol. 46, no. 1, pp. 83-94.

Kim, H. S.; Zhou, X.; Chattopadhyay, A. (2002): Interlaminar stress analysis of shell structures with piezoelectric patch including thermal loading. *AIAA Journal*, vol. 40, no. 12, pp. 2517-2525.

Marin, L.; Lesnic, D. (2007): The method of fundamental solutions for nonlinear functionally graded materials. *International Journal of Solids and Structures*, vol. 44, no. 21, pp. 6878-6890.

Ma, C. C.; Chang, S. W. (2004): Analytical exact solutions of heat conduction problems for anisotropic multi-layered media. *International Journal of Heat and Mass Transfer*, vol. 47, no. 8-9, pp. 1643-1655.

Ma, B. Y.; Dui, G. S.; Yang, S. Y.; Xin, L. B. (2015): The study of thermal stresses of a two phase FGM hollow sphere. *Computer Modeling in Engineering & Sciences*, vol. 109, no. 6, pp. 537-554.

Malekzadeh, P.; Ghaedsharaf, M. (2014): Three-dimensional thermoelastic analysis of finite length laminated cylindrical panels with functionally graded layers. *Meccanica*, vol. 49, pp. 887-906.

Malekzadeh, P.; Fiouz, A. R.; Razi, H. (2009): Three-dimensional dynamic analysis of laminated composite plates subjected to moving load. *Composite Structures*, vol. 90, pp. 105-114.

Malekzadeh, P.; Beni, A. A. (2015): Nonlinear free vibration of in-plane functionally graded rectangular plates. *Mechanics of Advanced Materials and Structures*, vol. 22, pp. 633-640.

Norouzi, M.; Delouei, A. A.; Seilsepour, M. (2013): A general exact solution for heat conduction in multilayer spherical composite laminates. *Composite Structures*, vol. 106, pp. 288-295.

Najafizadeh, M. M.; Eslami, M. R. (2002): First-order-theory-based thermoelastic stability of functionally graded material circular plates. *AIAA Journal*, vol. 40, no. 7, pp. 1444-1450.

Qian, H.; Zhou, D.; Liu, W. Q.; Fang, H. (2014): 3-D elasticity solutions of simply supported laminated rectangular plates in uniform temperature field. *Journal of Thermal Stresses*, vol. 37, no. 6, pp. 661-677.

Qian, H.; Zhou, D.; Liu, W. Q.; Fang, H.; Lu, W. D. (2015): 3-D elasticity solutions of layered rectangular plates subjected to thermo-loads. *Journal of Thermal Stresses*, vol. 38, no. 4, pp. 377-398.

Qian, H.; Zhou, D.; Liu, W. Q.; Fang, H.; Lu, W. D. (2015): Elasticity solution of simply supported laminated cylindrical arches subjected to thermo-loads. *Composite Structures*, vol. 131, pp. 273-281.

Ruhi, M.; Angoshtari, A.; Naghdabadi, R. (2005): Thermoelastic analysis of thick-walled finite-length cylinders of functionally graded materials. *Journal of Thermal Stresses*, vol. 28, no. 4, pp. 391-408.

Reddy, J. N.; Cheng, Z. Q. (2001): Three-dimensional thermomechanical deformations of functionally graded rectangular plates. *European Journal of Mechanics-A/Solids*, vol. 20, no. 5, pp. 841-855.

Rahideh, H.; Malekzadeh, P.; Haghighi, M. R. G. (2012): Heat conduction analysis of multi-layered FGMs considering the finite heat wave speed. *Energy Conversion and Management*, vol. 55, pp. 14-19.

Shiah, Y. C.; Guao, T. L.; Tan, C. L. (2005): Two-dimensional BEM thermoelastic analysis of anisotropic media with concentrated heat sources. *Computer Modeling in Engineering & Sciences*, vol. 7, no. 3, pp. 321-338.

Sladek, J.; Sladek, V.; Solek, P.; Wen, P. H.; Atluri, S. N. (2008): Thermal analysis of Reissner-Mindlin Shallow shells with FGM properties by the MLPG. *Computer Modeling in Engineering & Sciences*, vol. 30, no. 2, pp. 77-97.

Tarn, J. Q.; Wang, Y. M. (2003): Heat conduction in a cylindrically anisotropic tube of a functionally graded material. *Journal of Mechanics*, vol. 19, no. 3, pp. 365-372.

Talebitooti, M. (2013): Three-dimensional free vibration analysis of rotating laminated conical shells: layerwise differential quadrature (LW-DQ) method. *Archive of Applied Mechanics*, vol. 83, pp. 765-781.

Wu, L. H.; Jiang, Z. Q.; Liu, J. (2005): Thermoelastic stability of functionally graded cylindrical shells. *Composite Structures*, vol. 70, no. 1, pp. 60-68.

Wu, C. P.; Chi, Y. W. (2004): A refined asymptotic theory for the nonlinear analysis of laminated cylindrical shells. *Computers, Materials & Continua*, vol. 1, no. 4, pp. 337-352.

Wu, C. P.; Chiu, K. H.; Wang, Y. M. (2008): A differential reproducing kernel particle method for the analysis of multilayered elastic and piezoelectric plates. *Computer Modeling in Engineering & Sciences*, vol. 27, no. 3, pp. 163-186.

Xiang, Y.; Ma, Y. F.; Kitiornchai, S.; Lim, C. W.; Lau, C. W. H. (2002): Exact solutions for vibration of cylindrical shells with intermediate ring supports. *International Journal of Mechanical Sciences*, vol. 44, pp. 1907-1924.

Yas, M. H.; Aragh, B. S. (2010): Three-dimensional analysis for thermoelastic response of functionally graded fiber reinforced cylindrical panel. *Composite Structures*, vol. 92, no. 10, pp. 2391-2399.

Yuan, F. G. (1993): Thermal-stresses in thick laminated composite shells. *Composite Structures*, vol. 26, no. 1-2, pp. 63-75.

Zuo, H.; Yang, Z. B.; Chen, X. F.; Xie, Y.; Zhang, X. W. (2014): Bending, free vibration and buckling analysis of functionally graded plates via wavelet finite element method. *Computers, Materials & Continua*, vol. 44, no. 3, pp. 167-204.

Appendix A.

$$\left[R_{n0}^{i}(r)\right]=\begin{bmatrix}U_{n0}^{i}(r)\\V_{n0}^{i}(r)\\W_{n0}^{i}(r)\\Z_{n0}^{i}(r)\\X_{n0}^{i}(r)\\Y_{n0}^{i}(r)\end{bmatrix},\ \left[R_{mn1}^{i}(r)\right]=\begin{bmatrix}U_{mn1}^{i}(r)\\V_{mn1}^{i}(r)\\W_{mn1}^{i}(r)\\Z_{mn1}^{i}(r)\\X_{mn1}^{i}(r)\\Y_{mn1}^{i}(r)\end{bmatrix},\quad \left[R_{mn2}^{i}(r)\right]=\begin{bmatrix}U_{mn2}^{i}(r)\\V_{mn2}^{i}(r)\\W_{mn2}^{i}(r)\\Z_{mn2}^{i}(r)\\X_{mn2}^{i}(r)\\Y_{mn2}^{i}(r)\end{bmatrix},$$

$$\left[E_{n0}^{i}(r)\right]=\begin{bmatrix}e^{s_{01}^{i}r} & e^{s_{02}^{i}r}\\0 & 0\\\zeta_{01}^{i}e^{s_{01}^{i}r} & \zeta_{02}^{i}e^{s_{02}^{i}r}\\e^{s_{01}^{i}r}[(\lambda_i+2G_i)S_{01}^{i}+\dfrac{\lambda_i}{r_{i0}}-\dfrac{n\pi\lambda_i}{l}\zeta_{01}^{i}] & e^{s_{02}^{i}r}[(\lambda_i+2G_i)S_{02}^{i}+\dfrac{\lambda_i}{r_{i0}}-\dfrac{n\pi\lambda_i}{l}\zeta_{02}^{i}]\\G_i e^{s_{01}^{i}r}\left(\dfrac{n\pi}{l}+\zeta_{01}^{i}S_{01}^{i}\right) & G_i e^{s_{02}^{i}r}\left(\dfrac{n\pi}{l}+\zeta_{02}^{i}S_{02}^{i}\right)\\0 & 0\end{bmatrix}$$

$$\begin{bmatrix}e^{s_{03}^{i}r} & e^{s_{04}^{i}r}\\0 & 0\\\zeta_{03}^{i}e^{s_{03}^{i}r} & \zeta_{04}^{i}e^{s_{04}^{i}r}\\e^{s_{03}^{i}r}[(\lambda_i+2G_i)S_{03}^{i}+\dfrac{\lambda_i}{r_{i0}}-\dfrac{n\pi\lambda_i}{l}\zeta_{03}^{i}] & e^{s_{04}^{i}r}[(\lambda_i+2G_i)S_{04}^{i}+\dfrac{\lambda_i}{r_{i0}}-\dfrac{n\pi\lambda_i}{l}\zeta_{04}^{i}]\\G_i e^{s_{03}^{i}r}\left(\dfrac{n\pi}{l}+\zeta_{03}^{i}S_{03}^{i}\right) & G_i e^{s_{04}^{i}r}\left(\dfrac{n\pi}{l}+\zeta_{04}^{i}S_{04}^{i}\right)\\0 & 0\end{bmatrix}$$

$$\begin{bmatrix}0 & 0\\e^{s_{05}^{i}r} & e^{s_{06}^{i}r}\\0 & 0\\0 & 0\\0 & 0\\G_i e^{s_{05}^{i}r}\left(s_{05}^{i}-\dfrac{1}{r_{i0}}\right) & G_i e^{s_{06}^{i}r}\left(s_{06}^{i}-\dfrac{1}{r_{i0}}\right)\end{bmatrix},$$

$$\left[\Delta_{n0}^{i}\right]=\begin{bmatrix}a_{01}^{i}\\a_{02}^{i}\\a_{03}^{i}\\a_{04}^{i}\\a_{05}^{i}\\a_{06}^{i}\end{bmatrix},\ \left[Q_{n0}^{i}(r)\right]=\begin{bmatrix}0 & 0\\0 & 0\\-\dfrac{(3\lambda+2G)\alpha_i l}{(\lambda+G)n\pi}e^{\alpha_n^i r} & -\dfrac{(3\lambda+2G)\alpha_i l}{(\lambda+G)n\pi}e^{\beta_n^i r}\\-\dfrac{(3\lambda_i+2G_i)}{(\lambda_i+G_i)}G_i\alpha_i e^{\alpha_n^i r} & -\dfrac{(3\lambda_i+2G_i)}{(\lambda_i+G_i)}G_i\alpha_i e^{\beta_n^i r}\\-\dfrac{(3\lambda_i+2G_i)}{(\lambda_i+G_i)}\dfrac{G_i\alpha_i\alpha_n^i l}{n\pi}e^{\alpha_n^i r} & -\dfrac{(3\lambda_i+2G_i)}{(\lambda_i+G_i)}\dfrac{G_i\alpha_i\beta_n^i l}{n\pi}e^{\beta_n^i r}\\0 & 0\end{bmatrix}\begin{bmatrix}H_{ni}^{1}\\H_{ni}^{2}\end{bmatrix},$$

$$\left[E^i_{mn1}(r)\right]=\begin{bmatrix} e^{s^i_{11}r} & e^{s^i_{12}r} \\ \delta^i_{11}e^{s^i_{11}r} & \delta^i_{12}e^{s^i_{12}r} \\ \zeta^i_{11}e^{s^i_{11}r} & \zeta^i_{12}e^{s^i_{12}r} \\ e^{s^i_{11}r}\left[\left(\lambda_i+2G_i\right)S^i_{11}+\dfrac{m\lambda_i}{r_{i0}}\delta^i_{11}+\dfrac{\lambda_i}{r_{i0}}-\dfrac{n\pi\lambda_i}{l}\zeta^i_{11}\right] & e^{s^i_{12}r}\left[\left(\lambda_i+2G_i\right)S^i_{12}+\dfrac{m\lambda_i}{r_{i0}}\delta^i_{12}+\dfrac{\lambda_i}{r_{i0}}-\dfrac{n\pi\lambda_i}{l}\zeta^i_{12}\right] \\ G_ie^{s^i_{11}r}\left(\dfrac{n\pi}{l}+S^i_{11}\zeta^i_{11}\right) & G_ie^{s^i_{12}r}\left(\dfrac{n\pi}{l}+S^i_{12}\zeta^i_{12}\right) \\ G_ie^{s^i_{11}r}\left[-\dfrac{m}{r_{i0}}+\left(S^i_{11}-\dfrac{1}{r_{i0}}\right)\delta^i_{11}\right] & G_ie^{s^i_{12}r}\left[-\dfrac{m}{r_{i0}}+\left(S^i_{12}-\dfrac{1}{r_{i0}}\right)\delta^i_{12}\right] \end{bmatrix}$$

$$\begin{bmatrix} e^{s^i_{13}r} & e^{s^i_{14}r} \\ \delta^i_{13}e^{s^i_{13}r} & \delta^i_{14}e^{s^i_{14}r} \\ \zeta^i_{13}e^{s^i_{13}r} & \zeta^i_{14}e^{s^i_{14}r} \\ e^{s^i_{13}r}\left[\left(\lambda_i+2G_i\right)S^i_{13}+\dfrac{m\lambda_i}{r_{i0}}\delta^i_{13}+\dfrac{\lambda_i}{r_{i0}}-\dfrac{n\pi\lambda_i}{l}\zeta^i_{13}\right] & e^{s^i_{14}r}\left[\left(\lambda_i+2G_i\right)S^i_{14}+\dfrac{m\lambda_i}{r_{i0}}\delta^i_{14}+\dfrac{\lambda_i}{r_{i0}}-\dfrac{n\pi\lambda_i}{l}\zeta^i_{14}\right] \\ G_ie^{s^i_{13}r}\left(\dfrac{n\pi}{l}+S^i_{13}\zeta^i_{13}\right) & G_ie^{s^i_{14}r}\left(\dfrac{n\pi}{l}+S^i_{14}\zeta^i_{14}\right) \\ G_ie^{s^i_{13}r}\left[-\dfrac{m}{r_{i0}}+\left(S^i_{13}-\dfrac{1}{r_{i0}}\right)\delta^i_{13}\right] & G_ie^{s^i_{14}r}\left[-\dfrac{m}{r_{i0}}+\left(S^i_{14}-\dfrac{1}{r_{i0}}\right)\delta^i_{14}\right] \end{bmatrix}$$

$$\begin{bmatrix} e^{s^i_{15}r} & e^{s^i_{16}r} \\ \delta^i_{15}e^{s^i_{15}r} & \delta^i_{16}e^{s^i_{16}r} \\ \zeta^i_{15}e^{s^i_{15}r} & \zeta^i_{16}e^{s^i_{16}r} \\ e^{s^i_{15}r}\left[\left(\lambda_i+2G_i\right)S^i_{15}+\dfrac{m\lambda_i}{r_{i0}}\delta^i_{15}+\dfrac{\lambda_i}{r_{i0}}-\dfrac{n\pi\lambda_i}{l}\zeta^i_{15}\right] & e^{s^i_{16}r}\left[\left(\lambda_i+2G_i\right)S^i_{16}+\dfrac{m\lambda_i}{r_{i0}}\delta^i_{16}+\dfrac{\lambda_i}{r_{i0}}-\dfrac{n\pi\lambda_i}{l}\zeta^i_{16}\right] \\ G_ie^{s^i_{15}r}\left(\dfrac{n\pi}{l}+S^i_{15}\zeta^i_{15}\right) & G_ie^{s^i_{16}r}\left(\dfrac{n\pi}{l}+S^i_{16}\zeta^i_{16}\right) \\ G_ie^{s^i_{15}r}\left[-\dfrac{m}{r_{i0}}+\left(S^i_{15}-\dfrac{1}{r_{i0}}\right)\delta^i_{15}\right] & G_ie^{s^i_{16}r}\left[-\dfrac{m}{r_{i0}}+\left(S^i_{16}-\dfrac{1}{r_{i0}}\right)\delta^i_{16}\right] \end{bmatrix},$$

$$\left[\Delta^i_{mn1}\right]=\begin{bmatrix} a^i_{11} \\ a^i_{12} \\ a^i_{13} \\ a^i_{14} \\ a^i_{15} \\ a^i_{16} \end{bmatrix},\left[Q^i_{mn1}(r)\right]=\begin{bmatrix} 0 & 0 \\ 0 & 0 \\ -\dfrac{\left(3\lambda_i+2G_i\right)\alpha_i l}{\left(\lambda_i+G_i\right)n\pi}e^{\alpha^i_{mn}r} & -\dfrac{\left(3\lambda_i+2G_i\right)\alpha_i l}{\left(\lambda_i+G_i\right)n\pi}e^{\beta^i_{mn}r} \\ -\dfrac{\left(3\lambda_i+2G_i\right)}{\left(\lambda_i+G_i\right)}G_i\alpha_i e^{\alpha^i_{mn}r} & -\dfrac{\left(3\lambda_i+2G_i\right)}{\left(\lambda_i+G_i\right)}G_i\alpha_i e^{\beta^i_{mn}r} \\ -\dfrac{\left(3\lambda_i+2G_i\right)}{\left(\lambda_i+G_i\right)}\dfrac{G_i\alpha_i\alpha^i_{mn}l}{n\pi}e^{\alpha^i_{mn}r} & -\dfrac{\left(3\lambda_i+2G_i\right)}{\left(\lambda_i+G_i\right)}\dfrac{G_i\alpha_i\beta^i_{mn}l}{n\pi}e^{\beta^i_{mn}r} \\ 0 & 0 \end{bmatrix}\begin{bmatrix} H^3_{mni} \\ H^4_{mni} \end{bmatrix},$$

$$\left[E^i_{mn2}(r)\right]=\begin{bmatrix} e^{s^i_{21}r} & e^{s^i_{22}r} \\ \delta^i_{21}e^{s^i_{21}r} & \delta^i_{22}e^{s^i_{22}r} \\ \zeta^i_{21}e^{s^i_{21}r} & \zeta^i_{22}e^{s^i_{22}r} \\ e^{s^i_{21}r}[(\lambda_i+2G_i)S^i_{21}-\dfrac{m\lambda_i}{r_{i0}}\delta^i_{21}+\dfrac{\lambda_i}{r_{i0}}-\dfrac{n\pi\lambda_i}{l}\zeta^i_{21}] & e^{s^i_{22}r}[(\lambda_i+2G_i)S^i_{22}-\dfrac{m\lambda_i}{r_{i0}}\delta^i_{22}+\dfrac{\lambda_i}{r_{i0}}-\dfrac{n\pi\lambda_i}{l}\zeta^i_{22}], \\ G_ie^{s^i_{21}r}\left(\dfrac{n\pi}{l}+S^i_{21}\zeta^i_{21}\right) & G_ie^{s^i_{22}r}\left(\dfrac{n\pi}{l}+S^i_{22}\zeta^i_{22}\right) \\ G_ie^{s^i_{21}r}\left[\dfrac{m}{r_{i0}}+\left(S^i_{21}-\dfrac{1}{r_{i0}}\right)\delta^i_{21}\right] & G_ie^{s^i_{22}r}\left[\dfrac{m}{r_{i0}}+\left(S^i_{22}-\dfrac{1}{r_{i0}}\right)\delta^i_{22}\right] \end{bmatrix}$$

$$\begin{bmatrix} e^{s^i_{23}r} & e^{s^i_{24}r} \\ \delta^i_{23}e^{s^i_{23}r} & \delta^i_{24}e^{s^i_{24}r} \\ \zeta^i_{23}e^{s^i_{23}r} & \zeta^i_{24}e^{s^i_{24}r} \\ e^{s^i_{23}r}[(\lambda_i+2G_i)S^i_{23}-\dfrac{m\lambda_i}{r_{i0}}\delta^i_{23}+\dfrac{\lambda_i}{r_{i0}}-\dfrac{n\pi\lambda_i}{l}\zeta^i_{23}] & e^{s^i_{24}r}[(\lambda_i+2G_i)S^i_{24}-\dfrac{m\lambda_i}{r_{i0}}\delta^i_{24}+\dfrac{\lambda_i}{r_{i0}}-\dfrac{n\pi\lambda_i}{l}\zeta^i_{24}] \\ G_ie^{s^i_{23}r}\left(\dfrac{n\pi}{l}+S^i_{23}\zeta^i_{23}\right) & G_ie^{s^i_{24}r}\left(\dfrac{n\pi}{l}+S^i_{24}\zeta^i_{24}\right) \\ G_ie^{s^i_{23}r}\left[\dfrac{m}{r_{i0}}+\left(S^i_{23}-\dfrac{1}{r_{i0}}\right)\delta^i_{23}\right] & G_ie^{s^i_{24}r}\left[\dfrac{m}{r_{i0}}+\left(S^i_{24}-\dfrac{1}{r_{i0}}\right)\delta^i_{24}\right] \end{bmatrix}$$

$$\begin{bmatrix} e^{s^i_{25}r} & e^{s^i_{26}r} \\ \delta^i_{25}e^{s^i_{25}r} & \delta^i_{26}e^{s^i_{26}r} \\ \zeta^i_{25}e^{s^i_{25}r} & \zeta^i_{26}e^{s^i_{26}r} \\ e^{s^i_{25}r}[(\lambda_i+2G_i)S^i_{25}-\dfrac{m\lambda_i}{r_{i0}}\delta^i_{25}+\dfrac{\lambda_i}{r_{i0}}-\dfrac{n\pi\lambda_i}{l}\zeta^i_{25}] & e^{s^i_{26}r}[(\lambda_i+2G_i)S^i_{26}-\dfrac{m\lambda_i}{r_{i0}}\delta^i_{26}+\dfrac{\lambda_i}{r_{i0}}-\dfrac{n\pi\lambda_i}{l}\zeta^i_{26}] \\ G_ie^{s^i_{25}r}\left(\dfrac{n\pi}{l}+S^i_{25}\zeta^i_{25}\right) & G_ie^{s^i_{26}r}\left(\dfrac{n\pi}{l}+S^i_{26}\zeta^i_{26}\right) \\ G_ie^{s^i_{25}r}\left[\dfrac{m}{r_{i0}}+\left(S^i_{25}-\dfrac{1}{r_{i0}}\right)\delta^i_{25}\right] & G_ie^{s^i_{26}r}\left[\dfrac{m}{r_{i0}}+\left(S^i_{26}-\dfrac{1}{r_{i0}}\right)\delta^i_{26}\right] \end{bmatrix},$$

$$\left[\Delta^i_{mn2}\right]=\begin{bmatrix} a^i_{21} \\ a^i_{22} \\ a^i_{23} \\ a^i_{24} \\ a^i_{25} \\ a^i_{26} \end{bmatrix},\left[Q^i_{mn2}(r)\right]=\begin{bmatrix} 0 & 0 \\ 0 & 0 \\ -\dfrac{(3\lambda_i+2G_i)\alpha_i l}{(\lambda_i+G_i)n\pi}e^{\alpha^i_{mn}r} & -\dfrac{(3\lambda_i+2G_i)\alpha_i l}{(\lambda_i+G_i)n\pi}e^{\beta^i_{mn}r} \\ -\dfrac{(3\lambda_i+2G_i)}{(\lambda_i+G_i)}G_i\alpha_i e^{\alpha^i_{mn}r} & -\dfrac{(3\lambda_i+2G_i)}{(\lambda_i+G_i)}G_i\alpha_i e^{\beta^i_{mn}r} \\ -\dfrac{(3\lambda_i+2G_i)}{(\lambda_i+G_i)}\dfrac{G_i\alpha_i\alpha^i_{mn}l}{n\pi}e^{\alpha^i_{mn}r} & -\dfrac{(3\lambda_i+2G_i)}{(\lambda_i+G_i)}\dfrac{G_i\alpha_i\beta^i_{mn}l}{n\pi}e^{\beta^i_{mn}r} \\ 0 & 0 \end{bmatrix}\begin{bmatrix} H^5_{mni} \\ H^6_{mni} \end{bmatrix}.$$

Appendix B.

$$\begin{bmatrix} \nabla^{11}_{n0} & \nabla^{12}_{n0} \\ \nabla^{21}_{n0} & \nabla^{22}_{n0} \end{bmatrix}=\left\{\prod_{i=1}^{N}\left[E^i_{n0}(r_i)\right]\left[E^i_{n0}(r_{i-1})\right]^{-1}\right\},$$

$$\begin{bmatrix}\Omega_{n0}^{1}\\ \Omega_{n0}^{2}\\ \Omega_{n0}^{3}\\ \Omega_{n0}^{4}\\ \Omega_{n0}^{5}\\ \Omega_{n0}^{6}\end{bmatrix}=-\left\{\prod_{i=1}^{N}\left[E_{n0}^{i}\left(r_i\right)\right]\left[E_{n0}^{i}\left(r_{i-1}\right)\right]^{-1}\right\}\left[Q_{n0}^{1}\left(r_0\right)\right]$$

$$+\sum_{j=2}^{N}\left\{\prod_{i=j}^{N}\left[E_{n0}^{i}\left(r_i\right)\right]\left[E_{n0}^{i}\left(r_{i-1}\right)\right]^{-1}\right\}\left\{\left[Q_{n0}^{j\text{-}1}\left(r_{(j-1)}\right)\right]-\left[Q_{n0}^{j}\left(r_{(j-1)}\right)\right]\right\}+\left[Q_{n0}^{N}\left(r_N\right)\right],$$

$$\begin{bmatrix}\nabla_{mn1}^{11} & \nabla_{mn1}^{12}\\ \nabla_{mn1}^{21} & \nabla_{mn1}^{22}\end{bmatrix}=\left\{\prod_{i=1}^{N}\left[E_{mn1}^{i}\left(r_i\right)\right]\left[E_{mn1}^{i}\left(r_{i-1}\right)\right]^{-1}\right\},$$

$$\begin{bmatrix}\Omega_{mn1}^{1}\\ \Omega_{mn1}^{2}\\ \Omega_{mn1}^{3}\\ \Omega_{mn1}^{4}\\ \Omega_{mn1}^{5}\\ \Omega_{mn1}^{6}\end{bmatrix}=-\left\{\prod_{i=1}^{N}\left[E_{mn1}^{i}\left(r_i\right)\right]\left[E_{mn1}^{i}\left(r_{i-1}\right)\right]^{-1}\right\}\left[Q_{mn1}^{1}\left(r_0\right)\right]$$

$$+\sum_{j=2}^{N}\left\{\prod_{i=j}^{N}\left[E_{mn1}^{i}\left(r_i\right)\right]\left[E_{mn1}^{i}\left(r_{i-1}\right)\right]^{-1}\right\}\left\{\left[Q_{mn1}^{j-1}\left(r_{(j-1)}\right)\right]-\left[Q_{mn1}^{j}\left(r_{(j-1)}\right)\right]\right\}+\left[Q_{mn1}^{N}\left(r_N\right)\right],$$

$$\begin{bmatrix}\nabla_{mn2}^{11} & \nabla_{mn2}^{12}\\ \nabla_{mn2}^{21} & \nabla_{mn2}^{22}\end{bmatrix}=\left\{\prod_{i=1}^{N}\left[E_{mn2}^{i}\left(r_i\right)\right]\left[E_{mn2}^{i}\left(r_{i-1}\right)\right]^{-1}\right\},$$

$$\begin{bmatrix}\Omega_{mn2}^{1}\\ \Omega_{mn2}^{2}\\ \Omega_{mn2}^{3}\\ \Omega_{mn2}^{4}\\ \Omega_{mn2}^{5}\\ \Omega_{mn2}^{6}\end{bmatrix}=-\left\{\prod_{i=1}^{N}\left[E_{mn2}^{i}\left(r_i\right)\right]\left[E_{mn2}^{i}\left(r_{i-1}\right)\right]^{-1}\right\}\left[Q_{mn2}^{1}\left(r_0\right)\right]$$

$$+\sum_{j=2}^{N}\left\{\prod_{i=j}^{N}\left[E_{mn2}^{i}\left(r_i\right)\right]\left[E_{mn2}^{i}\left(r_{i-1}\right)\right]^{-1}\right\}\left\{\left[Q_{mn2}^{j-1}\left(r_{(j-1)}\right)\right]-\left[Q_{mn2}^{j}\left(r_{(j-1)}\right)\right]\right\}+\left[Q_{mn2}^{N}\left(r_N\right)\right].$$

where ∇_{n0}^{ij}, ∇_{mn1}^{ij} and ∇_{mn2}^{ij} $(i, j=1, 2)$ are the 3×3 matrices.